

SEGMENT STATURE HASH TABLE BASED COST EFFICIENT DATA SHARING IN CLOUD ENVIRONMENT

K. KarthikaLekshmi¹, Dr. M. Vigilsonprem²

¹ Assistant Professor, Department of Information Technology, Cape Institute of Technology

² Professor, Department of Computer Science and Engineering, R.M.D. Engineering College

ABSTRACT

Data sharing for dynamic groups is a promising approach that anonymously shares the data with others. Though, anonymity and traceability for sharing the data was provided in cloud environments, storage overhead with integrity and encryption computation cost remained constant. In this work, a framework called Cryptographic Multi-linear Data Sharing for Dynamic Group (CMDS-DG) is addressed to reduce the storage overhead, encryption computation cost and to maintain privacy on adding new users in a cloud environment. The cryptographic based data sharing on dynamic cloud service use RepeatKeyRotate Encryption to maintain higher privacy level. The performance results show that the CMDS-DG framework can significantly reduce the encryption computation cost by minimizing the storage overhead and maintains a higher privacy level with other data sharing methods.

Keywords: CMDS-DG, SSHT, Multi-linear Data Sharing

I. INTRODUCTION

A Cloud [9] is a type of parallel and distributed system consisting of a collection of interconnected and virtualized computers that are dynamically provisioned and presented as one or more unified computing resources based on service-level agreements established through negotiation between the service provider and consumers. Types of the cloud model include public, private, community and hybrid clouds [4]. The characteristics provided by the cloud computing include independent resource pooling, on-demand self-service, elasticity, pay-per-use, virtualization, increased storage and trust worthy metering service, etc.. To implement these features; cloud computing systems offer services at various levels, from the bottom layer to the top layer. Infrastructure-as-a-Service (IaaS) is offered in the bottom layer, which delivers services in the forms of storage, network, and computational capability. Platform as a Service (PaaS) is the middle layer which delivers services in the form of environment for software execution. Software as a Service (SaaS) locates in the top layer, which offers software applications as a service. In general, cloud computing is built over the three minimum level technologies, which includes web applications and web services, virtualization techniques for both hardware and software, cryptographic techniques for data security.

The remaining part of this paper is organized as follows. In Section II, security related works while sharing the data had been presented. Then, Section III discusses the Structural framework of Cryptographic Multi-linear Data Sharing for Dynamic Group (CMDS-DG). Impact of encryption computation cost and storage overhead are

given in Section IV. Finally, the conclusion is given in section V.

II. RELATED WORKS

With the incredible data and resource sharing in a cloud environment, both cloud owners and cloud users enjoy lower marginal cost than ever before. A secure multi-owner data sharing, called, Mona [1] was designed with the objective of providing security considering storage overhead and encryption computation cost. However, storage overhead with integrity and encryption computation cost remained constant. In Oruta [2], data sharing by preserving the privacy of data were provided using a third party auditor (TPA) without retrieving the entire file. But, it did not provide mechanisms to maintain privacy while adding new users into the cloud environment. Another secure sharing approach was provided in CyberLiveApp [3] with the objective of providing privacy to the shared data. Two main advantages of using CyberLivApp were ensuring application sharing and migration between Virtual Machines. However, flexible collaboration was not provided. Role Based Access Control (RBAC) mechanism [5] was introduced with the objective of increasing anonymity and improving user revocation through algebraic structure. However, a collaborative framework was not ensured. A dynamic audit service model was introduced in the paper [6] with the aid of an index - hash table and random sampling with the motive of reducing computation and storage overhead. But, scalability remained unsolved. In paper [7] auditing of data stored in a dynamic manner was addressed using index-hash table mechanism. Another method was designed in [8] against unauthorized access by integrating user behavior profile and decoy technology. Many existing issues still need refinements, including, cost of cryptographic operations, storage overhead, privacy-preserving access control etc. In the proposed work, a framework called Cryptographic Multi-linear Data Sharing for Dynamic Group (CMDS-DG) is presented. This framework handles multiple owners in the dynamic cloud environment.

III. Structural framework of Cryptographic Multi-Linear Data Sharing for Dynamic Group (CMDS-DG)

The structural framework of CMDS-DG is shown in Figure1. This framework includes three stages, namely Cryptographic Multi-linear Mapping, construction of Segment Stature Hash Table and Crptographic based Data Sharing between cloud users.

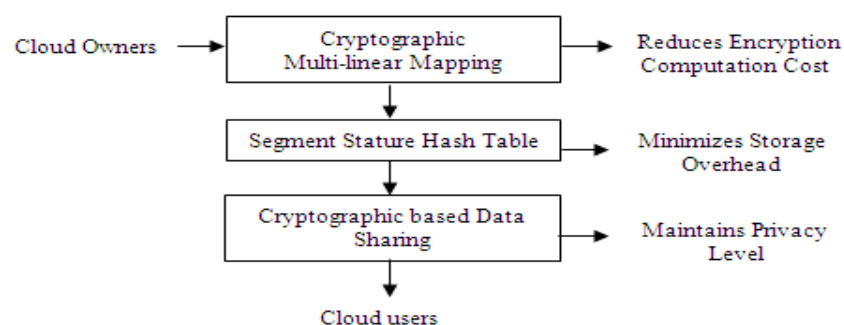


Figure 1. Framework of CMDS-DG

Two parameters Group operations and Mapping key are obtained in the proposed framework. Furthermore, the proposed framework uses a Hash based mechanism called Segment Stature Hash Table during data sharing in a

cloud environment. The elaborate description of each stage is explained in detail in the following sections.

3.1 Cryptographic Multi-linear Mapping

The framework CMDS-DG provides a Cryptographic Multi-linear Mapping to ensure that security is provided with minimized encryption computation cost. When compared to the conventional cryptographic bilinear mapping that offers pairing between two cloud users, the cryptographic multi-linear mapping ensures data sharing between multi-owners and many cloud users.

Let us assume the cloud owners as ' CO_1, CO_2, \dots, CO_n ' of order ' p ' with cloud service provider ' CSP_1 ', then Cryptographic Multi-linear Mapping is formalized as

$$CO_a * CO_b \rightarrow CO_{a+b} \text{ for } (a + b) \leq n \tag{1}$$

Where a, b are two different cloud owners, which contains dissimilar files or data, n represents the number of data or file contained by the cloud owners.

From (1) group operations between cloud owners ' CO_a ' and ' CO_b ' is performed in an efficient manner. Let us assume that ' $p, q \in CO_i$ ' then ' $sum(func, i, p, q)$ ' measures ' $p + q \in CO_i$ ' whereas ' $sub(func, i, p, q)$ ' measures ' $p - q \in CO_i$ '. Here p and q are data retrieved from a particular cloud owner. To share data between four cloud users ' CU_1, CU_2, CU_3, CU_4 ', they form the group a, b, c, d and broadcast $G_1^a, G_2^b, G_3^c, G_4^d$ using the mapping key.

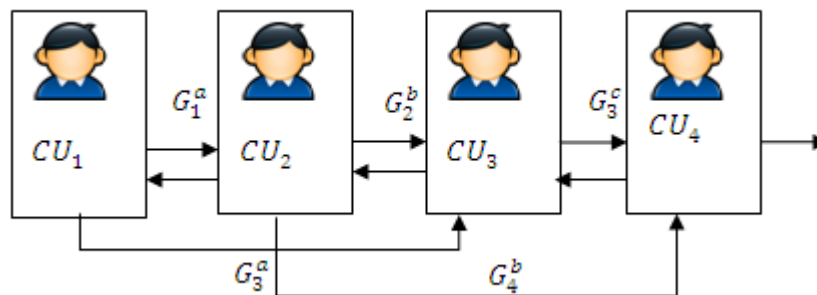


Figure 2. Design of Cryptographic Multi-linear Mapping

The mapping key for data sharing between ' G_1, G_2 ' and ' G_2, G_4 ' is formalized as given below

$$MK_{1,2} = (G_1, G_2) = G_1^a \tag{2}$$

$$MK_{2,4} = (G_2, G_4) = G_2^b \tag{3}$$

Where a, b, c and d are group names. As illustrated in the above figure 2, data sharing between cloud users are performed through mapping key ' MK '.

3.2 Segment Stature Hash Table (SSHT)

Once efficient data sharing between multi-users are performed, efficient handling of storage has to be performed to reduce the storage overhead. The objective behind the application of Segment Stature Hash Table is the efficient mapping of each key to only one hash value. Due to this, multi-linear mapping is efficiently performed by applying Segment Stature Hash Table. In addition, the storage overhead during data sharing is also reduced because only the encrypted file is shared with others.

The Segment Stature Hash Table consists of a table with three fields, namely Cloud Owner ID no, Group Value, Mapping Key generated for each cloud user.

Table 1. Segment Stature Hash Table

Content	Description
CO_ID	Cloud Owner ID no (CO_1, CO_2, CO_3, CO_4) and so on
G_V	Group Value ($G_1^a, G_2^b, G_3^c, G_4^d$) and so on
M_Key	Mapping Key generated for each cloud user $MK_{1,2}, MK_{3,4}$ and so onk

3.3 Cryptographic Based Data Sharing

Cryptographic based data sharing is performed using RepeatKeyRotate Encryption Algorithm. The algorithmic steps are listed below

//Algorithm – RepeatKeyRotate Encryption

Input: Cloud Owner ID No, Group Value, File

Output: File sharing between multiple owners.

Initialize the cloud owner with file to be sent

Let the cloud owner ID No be ‘CO_i’

Let the file to be sent by ‘CO_i’ be ‘File_i’

For all CO - ID_i

For all G - V_i

Generate mapping key *M - Key_i* for data sharing using (4)

Encrypted file $EFile_i = (M - Key_i | File_i)$

Encrypted file *EFile_i* is shared between multi-owners

End For

End For

As given in the algorithm, initially, the cloud owner who wants to share the file or data with others is initialized with the Cloud Owner ID no and Group Value. The generated Mapping Key for each cloud users from SSHT is also extracted. Based on the mapping key for each cloud owner, encryption is performed with the motive of reducing the storage overhead. By obtaining separate keys for each cloud owner, higher amount of privacy is maintained.

IV. EXPERIMENTAL SETUP

The proposed framework is tested and the outcome is discussed in this section. Extensive simulations using Cloudsim are conducted to measure and evaluate the efficiency of the proposed framework. Based on the results, the impacts of two parameters, namely, encryption computation cost and storage overhead are illustrated. Each instance type is configured with a specific amount of memory, CPUs, and local storage. This

type is equipped with two quad core 2.33-2.66 GHz Xeon processors (8 cores total), 7 GB RAM, and 1690 GB local disk storage.

Cryptographic Multi-linear Data Sharing for Dynamic Group is compared with the existing Multi-Owner Data Sharing for Dynamic Groups in the Cloud (MONA) [1] and Privacy-Preserving Public Auditing for Shared Data in the Cloud (ORUTA) [2].

4.1 Impact of Privacy

In table 2 we compare the privacy of the proposed framework using the RepeatKeyRotate Encryption on multi-owner data sharing. The experiments were conducted using varied number of cloud owners and cloud users, which is measured in terms of percentage (%).

$$\text{Privacy (\%)} = (\text{Data Retrieved by cloud users (KB)} / \text{Data Requested by cloud user (KB)}) * 100$$

Methods	Privacy (%)
Mona	61
Oruta	70
CMDS-DG	77

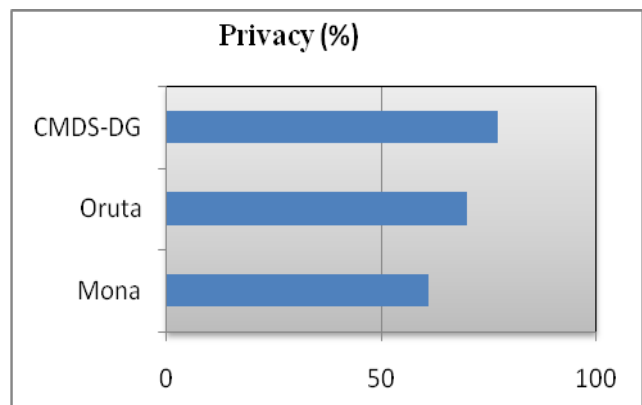


Table 2 Tabulation for Privacy

Figure3. Measure of Privacy

To explore the influence of privacy rate on CMDS-DG framework, the experiments were performed by applying 35 different cloud owners and 21 different cloud users from six different sequences obtained from allbookstores.com as depicted in figure3. The figure shows that the privacy reaches its zenith compared to two other methods because of the application of cryptographic based data sharing using a RepeatKeyRotate encryption algorithm. The application of the RepeatKeyRotate encryption algorithm efficiently extracts each key for different users which help in improving the privacy measure by 12.82 % when compared to Mona [1] and 6.41% when compared to Oruta [2] respectively.

4.2 Impact of Data Sharing Delivery Ratio

Finally, table 3 provides the data sharing delivery ratio of CMDS-DG framework for seven different cloud owners that is measured in terms of percentage (%). The Data sharing delivery ratio using CMDS-DG is the percentage ratio of data received by cloud users to the data sent by the cloud owners.

$$DSDR = \frac{\text{Data received by cloud users (KB)}}{\text{Data sent by cloud owners (KB)}} * 100$$

The data sharing delivery ratio between the 35 cloud owners and 21 cloud users for efficient data sharing in cloud environment is shown in Figure4. It shows that the proposed CMDS-DG framework potentially yields better results than existing Mona [1] and Oruta [2].

No. of cloud owners	Data sharing delivery ratio (%)		
	CMDS-DG	Mona	Oruta
5	80	70	60
10	83.3	75.25	69.23
15	85	80.13	71.43
20	75	68.35	62.36
25	72.8	65.22	55.19
30	74.55	69.13	61.32
35	80.25	72.33	64.81

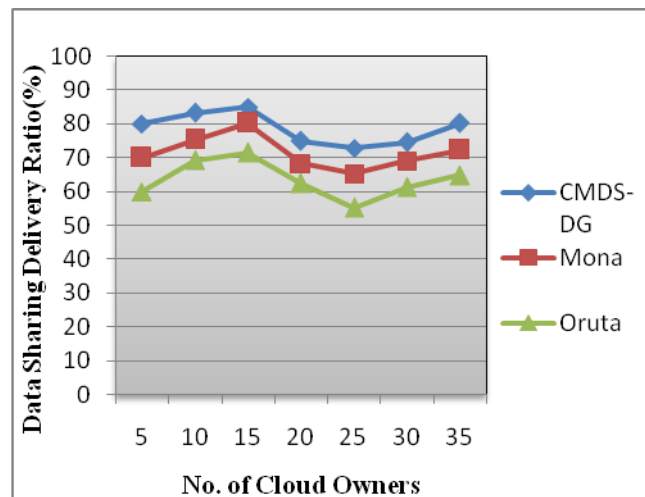


Table 3 Tabulation of Data Sharing Delivery Ratio **Figure4. Data Sharing Delivery Ratio (%)**

The CMDS-DG framework increases the data sharing delivery ratio between the cloud users and cloud owners by 5 – 12 % compared to Mona [1] and is improved by 15 – 25 % compared to Oruta [2].

V. CONCLUSION

In this work, a framework called, Cryptographic Multi-linear Data Sharing for Dynamic Group (CMDS-DG) is addressed to minimize the encryption computation cost and to reduce the storage overhead during data sharing between multiple cloud owners and cloud users. This work shows how encryption computation cost is reduced using the Cryptographic Multi-linear Mapping. It also shows how the storage overhead is reduced using Segment Stature Hash Table. We further show attainable performance gains of the proposed framework in terms of privacy and data sharing delivery ratio by applying RepeatKeyRotate Encryption. Performance results show that the proposed CMDS-DG framework provides comparatively better efficiency in terms of privacy and data sharing delivery ratio compared to state-of-art works.

REFERENCES

- [1] Xuefeng Liu, Yuqing Zhang, Member, Boyang Wang, and Jingbo Yan, “Mona: Secure Multi-Owner Data Sharing for Dynamic Groups in the Cloud,” IEEE Transactions on Parallel and Distributed Systems, Vol. 24, No. 6, June 2013.
- [2] Boyang Wang, Baochun Li, and Hui Li, “Oruta: Privacy-Preserving Public Auditing for Shared Data in the Cloud,” IEEE Transactions on Cloud Computing, Vol: 2, Issue: 1, 2014.
- [3] Jianxin Li, Yu Jia, Lu Liu, Tianyu Woa, “CyberLiveApp: A secure sharing and migration approach for live virtual desktop applications in a cloud environment,” Future Generation Computer Systems., Elsevier journal, 2013.
- [4] K.KarthikaLekshmi, Dr. E. Baburaj,”Data Integrity Issues in Cloud Storage System-A Survey,” International Journal of Digital Content Technology and its Applications, Vol.8, No.3, June 2014.

- [5] Yan Zhu, Gail-Joon Ahn, IEEE, Hongxin Hu, Di Ma, and Shanbiao Wang,” Role-Based Cryptosystem: A New Cryptographic RBAC System Based on Role-Key Hierarchy”, IEEE Transactions On Information Forensics And Security, Vol. 8, No. 12, December 2013.
- [6] Yan Zhu, Gail-Joon Ahn, Hongxin Hu, Stephen S. Yau, Ho G. An and Chang-Jun Hu,” Dynamic Audit Services for Outsourced Storages in Clouds”, IEEE Transactions On Services Computing, Vol. 6, No. 2, April-June 2013.
- [7] Rakhi Bhardwaj, Vikas Maral,” Dynamic Data Storage Auditing Services in Cloud Computing”, International Journal of Engineering and Advanced Technology (IJEAT) ISSN: 2249-8958, Volume-2, Issue-4, April 2013.
- [8] Salvatore J. Stolfo, Malek Ben Salem, Malek Ben Salem,” Fog Computing: Mitigating Insider Data Theft Attacks in the Cloud”, IEEE Computer Society, Feb 2012.
- [9] Rajkumar Buyya, Chee Shin Yeo and Srikumar, Venugopal, “Market-oriented cloud computing: Vision, hype, and reality for delivering IT services as computing utilities”, In Proceedings of the 10th IEEE International Conference on High Performance Computing and Communications, pp. 5-13, 2008.

UNDERSTANDING 'THE CIRCLE

Syed Abdul Lateef

Institution: Christ University, Bangalore. B.Sc 2nd Year,

ABSTRACT

Circle is cannot be a polygon because it does not have sides and is not a closed figure. But thinking of a polygon in a different way could result in a better understanding of circle and polygon. Thus this paper is the introduction of the new concept for polygons.

I. INTRODUCTION

In general it is said that circle is a polygon having infinite number of sides. This does not give any meaning because the term infinity (∞) itself do not have a definite meaning. Thus by not saying the term infinity, that is by thinking it in other terms the relation between the circle and the polygon could be found. This is the general explanation of the shapes known to us.

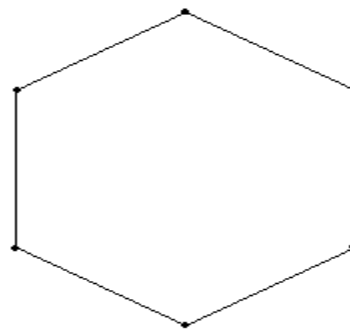
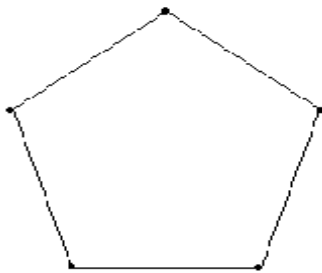
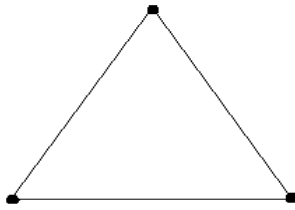
Circle is a simple shape in Euclidean geometry. It is the set of all points in a plane that are at a given distance from a given point, the centre; equivalently it is the curve traced out by a point that moves so that its distance from a given point is constant. The distance between any of the points and the centre is called the radius.

Polygon is a closed plane figure bounded by three or more straight sides that meet in pairs in the same number of vertices, and do not intersect other than at vertices. The two types of polygons (based on their sides) are regular and irregular polygons. Regular polygons are those having all sides equal and of course all angles are equal. The opposite to it is an irregular polygon.

II. CONCEPT OF EDGE IN POLYGON

We know that a polygon is a perfectly closed figure having sides. But not in terms of sides when a polygon is in terms of Edges, then it could be found more meaningful. Let us take the example of a triangle, which is a basic polygon. Generally we say 'A triangle is a polygon having three sides'. Instead of using the terms sides when we use Edges i.e. by saying 'A triangle is a polygon having three points (edges) connected by the shortest distance between them (maintaining the regularity between the edges) then the properties of the polygon could be understood more precisely.

2.1 Figures

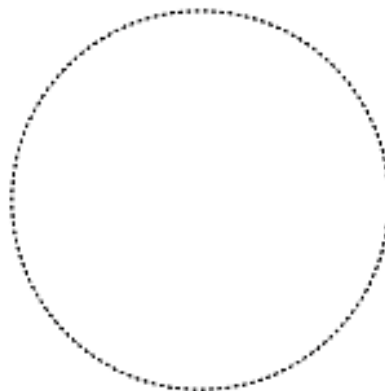


III. EXPLANATION FOR REGULAR AND IRREGULAR POLYGON

A regular polygon is a closed figure in which the edges are separated by equal distance in the regular intervals. Thus it satisfies the conditions having equal sides and angle. The irregular polygons have the edges separated by different distances resulting in different angles.

IV. CIRCLE AS A POLYGON

When the concept of edge is considered then the circle could be defined as a closed figure having edges separated by almost zero distance and are at an equal distance from a point (which is the centre of the circle). Thus the circle comes under the category of regular polygons.



V. COMPARING THE AREA OF CIRCLE AND POLYGON

The area of circle is πr^2 and the area of regular polygon is $A = n \frac{\sin \frac{360^\circ}{n} r^2}{2}$ (Where r is the Radius and n is the number of sides). According to the concept of edges circle is also one of the types of regular polygon the above areas are equal. The number of sides is equal to the number of edges. Thus

$$\pi r^2 = n \frac{\sin \frac{360^\circ}{n} r^2}{2}$$

$$\frac{2\pi}{n} = \sin \frac{360^\circ}{n}$$

$2\pi = 6.283$ (approximately) and n is a very large number the value of $\frac{2\pi}{n}$ lies between 0 and 1. Also the value of \sin lies between 0 and 1. The area of circle when considered as a regular polygon is same.

VI. CONCLUSION

Thus the concept of the edges concludes that the circle is one among the regular polygons.

VII. ACKNOWLEDGEMENT

I thank my friend Nikhil who helped to think me about this concept and thanks for the support of my family and friends.

EFFECT OF AUSTENITIZATION AND COOLING ON HARDENING OF X65 GRADE LINE-PIPE HSLA STEEL

Nidhi Garg, Sanjay Panwar

Department of Physics, Maharishi Markandeshwar University, Mullana Ambala, (India)

ABSTRACT

Studies were carried out on the effect of austenitization and cooling of line-pipe HSLA steel. Hardness measurements were conducted after quenching/cooling the steel. As a result of change in quenching/cooling media hardness could be significantly altered. Consequently fast cooling rates, such as quenching in water and oil lead to high hardness levels as compared to the air cooling. Metallographic examinations revealed decomposition of austenite into martensite and ferrite together with formation of fine precipitate particles within the ferrite matrix and segregation of coarse/fine precipitate particles along the lath boundaries.

Keywords: *HSLA Steel, Line-Pipe Steel, Austenitization, Quenching, Cooling*

I. INTRODUCTION

High-Strength Low-Alloy (HSLA) steels have been promising materials for various structural applications, viz., construction, automotive component, truck frames, crane booms, offshore drilling and line-pipe applications for transmission of oil and gas pipe-lines. X65 HSLA steel is being widely used for the line-pipe applications in oil and gas sectors. Over the past three decades, the world production of oil and gas and the consumption of their products have grown significantly, which caused an increase in the use of pipelines for their transport. Similarly, the use of pipelines for transporting iron ore over long distances has been a solution adopted by many mining companies. To meet this demand, it is necessary that the pipes used in transport have larger diameters and work at high pressures. The development of high strength steels, which avoid the use of very high wall thicknesses, makes a significant contribution to pipeline project cost reduction [1-8].

Microalloy additions to steels have been instrumental to the successful development of new steel products with enhanced property combinations. The extensive use of microalloyed flat rolled steels in pipeline plate products and automotive sheet steels, typically with microalloy additions of less than several hundredths of a weight percent, has become commonplace [10]. Many researchers and developers worked on microalloying steel elements and their outputs [9-17].

The first “pipelines” were laid in China about 1000 B.C., while the first oil pipeline was built in Baku, 1878, it was above 10 km long and 2” in diameter and it was realized to decrease the cost of transportation by above 90% [18]. The trend in the demand for large diameter pipe, in order to improve transportation capacity, is well established by the contemporary onshore energy industry. The need to achieve higher strength accompanied with sufficient toughness and ductility has pushed the development of high strength steels (HSS) aiming at performance and durability to operate in harsh environments. These new steel grades for high pressure purposes (between 12 to 20 MPa) can be seen as an advanced variant of HSLA steels. HSS steels typically contain very low carbon content and small amounts of alloying elements (microalloyed), such as Nb, V, Ti and Mo [19-22].

High strength steels such as American Petroleum Institute (API) 5L X70 and beyond, possesses highly refined grain and high cleanliness. They are characterized by the low sulfur content and reduced amount of detrimental second phases such as oxides, inclusions and pearlite.

II. EXPERIMENTAL DETAILS

Table 1 gives the chemical composition of the steels. In order to study the effect of quenching media, the X65 grade HSLA steel in the was given solution treatment 1000°C for 180 min, followed by quenching in water (WQ), oil (OQ) and cooling in air (AC).

Table 1 Chemical Composition (wt. pct.)

C	Mn	P	S	Si	Cu	Cr	Mo
0.06	1.66	0.009	0.005	0.28	0.06	0.11	0.26

Ni	Al	Co	Nb	V	Ti
0.26	0.032	0.007	0.059	0.025	0.014

Hardness measurements were carried out on a Vickers Hardness Testing machine (VM 50) by employing a 30 kgf load. The reported hardness values are the mean of at least ten indentations.

For metallographic examinations specimens were prepared by conventional polishing techniques. The polished specimens were etched with 2% nital (2% nitric acid and 98% methanol/ethanol). Optical microscopic examinations were conducted on an Inverted Metallographic Station (IMS-7001).

III. RESULTS

3.1 Hardness

Figure 1 shows the variation of hardness after various stages of quenching. Hardness increases with increasing rates of cooling. Accordingly, maximum hardness (253 HV₃₀) is obtained in water quenched condition. However, air cooling results in minimum hardness value (187 HV₃₀) in X65 grade HSLA steel.

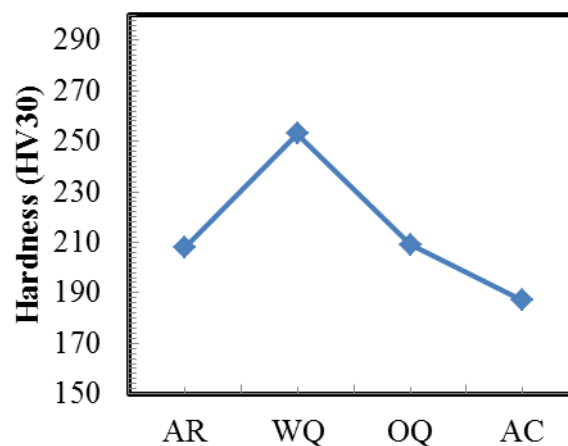


Figure 1. Variation of Hardness

3.2 Optical Microscopy

The steel in as-received condition consists of bands of ferrite and pearlite. As shown in Fig. 2 the alignment of bands along the flow lines are an indicative that the steel would have been given cold/hot rolling treatment.

Extensive metallographic examinations revealed transformation of austenite into ferrite and martensite after quenching. Figures 3-6 show the microstructural transformation in AR condition as well as after austenitization at 1000^oC followed by quenching in water, oil and air respectively. It has been observed that water quenching results in the formation of ferrite together with thick martensite laths (Figs. 3). However, oil quenching results in the formation of fine martensitic needles (Figs. 4). On the other hand air cooling results in primarily ferritic microstructure together with the formation a few coarse precipitate particles in the ferrite matrix (Figs. 5).

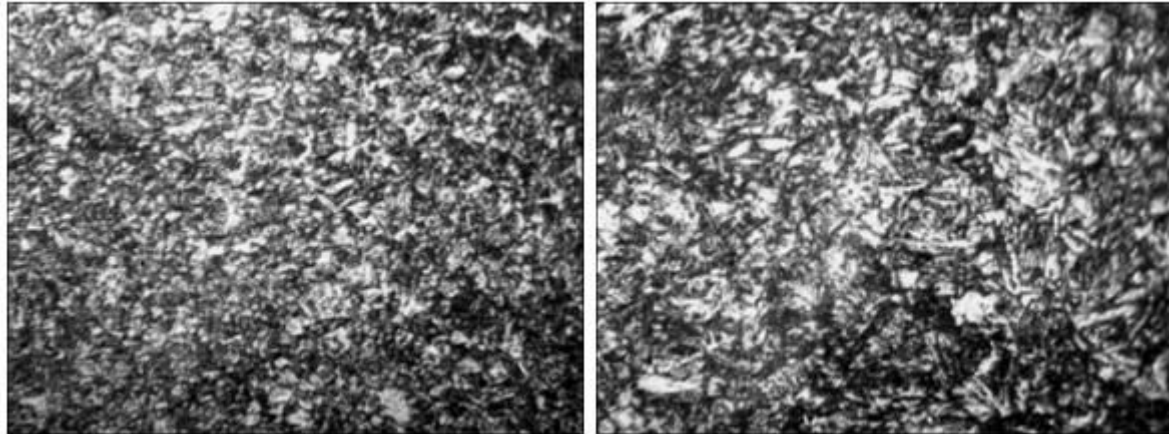


Figure 2. Optical Micrographs Showing Ferrite and Pearlite Bands in As-Received (AR) Condition

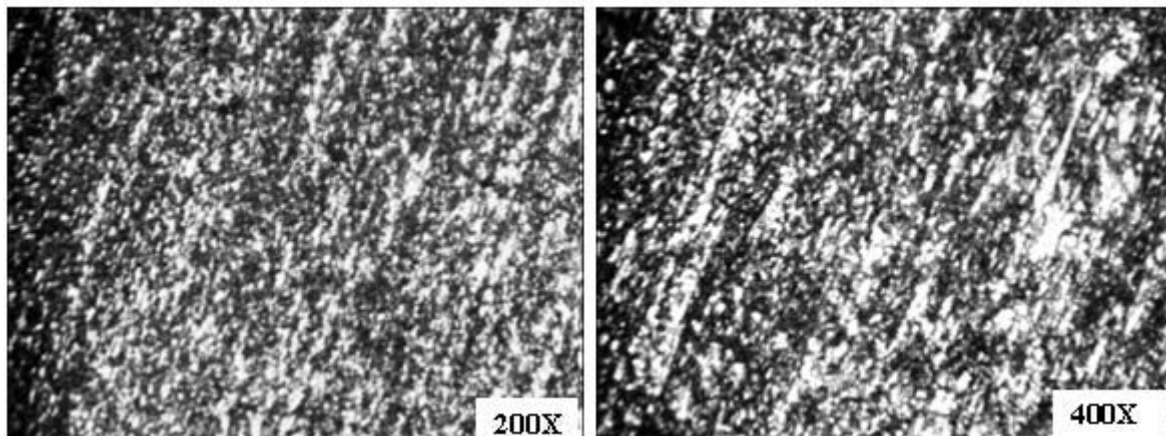


Figure 3. Optical Micrographs Showing Martensite Laths in WQ Condition

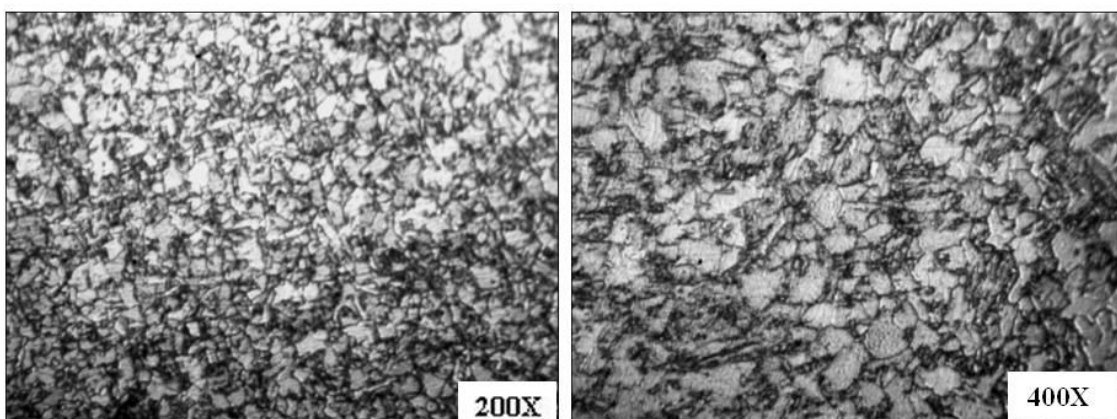


Figure 4. Optical Micrographs Showing Predominantly Polygonal Ferrite in OQ Condition

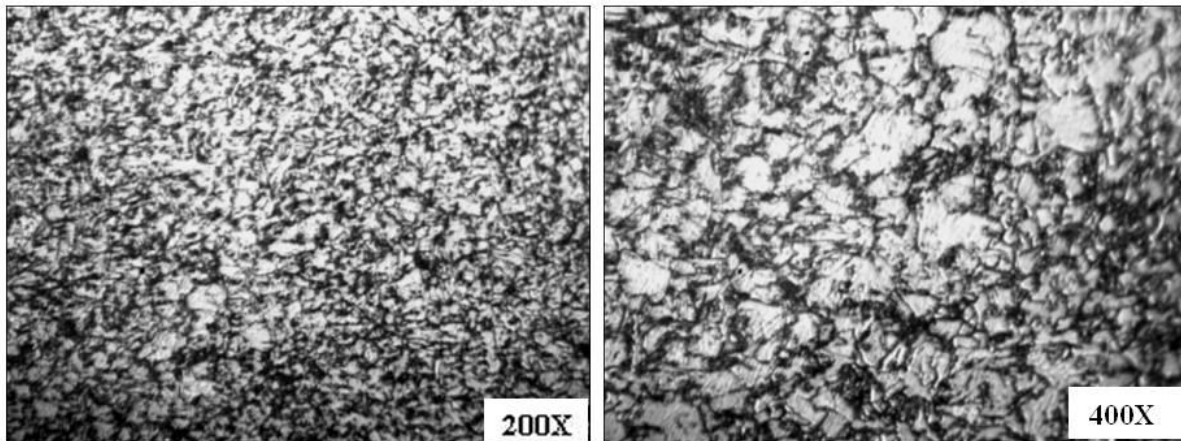


Figure 5. Optical Micrographs Showing Predominantly Ferrite with Coarse Precipitate Particles in AC Condition

IV. DISCUSSION

Heat-treatment of steel involves the transformation of austenite into ferrite with a low solubility of carbon. The carbon atoms segregate around grain boundaries to form martensite/cementite. This is accompanied by mobility or diffusion of the carbon atoms. The movements of atoms accelerated at high temperatures but increasingly sluggish as the temperature decreases. The increasing cooling rates, in general, reduce the time for structural transformations. Therefore, residual austenite transforms at lower temperatures, with smaller movements of atoms and results in finer structures. However, at lower temperatures ($< 250^{\circ}\text{C}$) another transition structure is formed owing to slow diffusion process.

The processing of HSLA steels play an important role in the tailoring of their mechanical properties associated with structural transformations. The hardening of steels is generally achieved by suitable quench from within or above the critical temperature region. Quenching in general, suppresses the transformation of austenite into ferrite and/or cementite, and to cause a partial decomposition to martensite at such a low temperature. This effect is attributed to the critical cooling velocity, which is greatly influenced by the existence of alloying elements, which therefore is responsible for hardening with mild quenching. Water is one of the most efficient quenching media when maximum hardness is desirable, but it causes distortion and cracking. The quenching velocity of oil is much lower than water. Intermediate rates between water and oil can be generally achieved with air cooling. Austenitizing temperature, cooling rates and alloy composition have been observed to affect the mechanical properties of HSLA steels via their influence on the microstructural transformation [3, 23-26].

Figure 3-5 illustrates the effect of cooling rates on microstructure after austenitization at 1000°C in commercial X65 grade HSLA steel. It has been observed that austenite decomposition accelerates with increasing cooling rates, thereby increasing the hardening effect. In other words, higher cooling rates leads to higher hardening as manifested by the transformation of austenite to ferrite and subsequently to martensite with increasing cooling rates (Fig. 1 and Fig. 3-5). The researchers in [3, 26] described the microstructural evolution during austenite decomposition in HSLA steel as a function of cooling rate. At higher cooling rates ($\sim 4300^{\circ}\text{C/s}$) austenite transforms to low-carbon martensite as can be manifested by the predominantly martensitic structure in water quenched condition after austenitization at 1000°C (Fig. 3). At cooling rates of ($\sim 1000^{\circ}\text{C/s}$), a microstructure referred to as acicular ferrite is formed (Fig. 4). However, at lower cooling rates ($< 1000^{\circ}\text{C/s}$) majority of the

austenite is transformed to polygonal ferrite as shown in Fig. 5. In earlier studies [16, 27] on the effect of cold work and aging of HSLA steels, it was observed that oil quenching from austenitic region lead to the decomposition of austenite into martensite and ferrite together with the segregation of fine carbide particles along the lath boundaries.

V. ACKNOWLEDGEMENT

The authors acknowledge the Department of Science & Technology, New Delhi for providing financial support (SR/FTP/ETA-044/2009) for the establishment of Material Science Research Lab.

REFERENCES

- [1]. H.G. Hillenbrand, M. Gräf and C. Kalwa, Development and production of high strength pipeline steels. in: Niobium Science & Technology. TMS; 2001, 543-569.
- [2]. H.G. Hillenbrand and C. Kalwa, Production and service behavior of high strength large diameter pipe. in: Proceedings of the International Conference on Application and Evaluation of High Grade Line pipes in Hostile Environments; 2002. EUROPIPE; 2002, 1-17.
- [3]. A.D. Wilson, E.G. Hamburg, D.J. Colvin, S.W. Thompson, and G. Krauss: Proc. Int. Conf. on Microalloyed HSLA Steel, Microalloying '88, ASM International, Metals Park, OH, 1988, 259-275.
- [4]. C. Kalwa, H.G. Hillenbrand and M. Gräf: High strength steel pipes – new developments and applications, in Proceedings of the Onshore Pipeline Conference. EUROPIPE; 2002, 1-12.
- [5]. M. Gräf, H. G. Hillenbrand, C. J. Heckmann and K. A. Niederhoff: High-strength large-diameter pipe for long-distance high pressure gas pipelines. In: Proceedings of the 13th International Offshore and Polar Engineering Conference, EUROPIPE; PMid: 12764765, 2003, 97-104.
- [6]. L. Li and L. Xu, Designing with High-Strength Low-Alloy Steels. In: Handbook of Mechanical Alloy Design. Marcel Dekker, Inc. PMCID: PMC3090257, 2004, 249-320.
- [7]. M.J. Gray and F. Siciliano, High Strength Microalloyed Line pipe steels: Half a Century of Evolution. Microalloyed Steel Institute; PMid: 19106795, 2009, 20-45.
- [8]. F. Barbaro, L. Fletcher, C. Dinnis, J. Piper and J.M. Gray, Design and specification of line pipe and line pipe steels for weldability, constructability and integrity, in: Proceedings of the 18th JTM on Pipeline Research. PRCI/AFIA/EPRG; 2011, 1-21
- [9]. F.B. Pickering, "High-Strength, Low-Alloy Steels - A Decade of Progress" Microalloying '75, Union Carbide Corp., New York, 1977, 9-31.
- [10]. S. G. Hong, K. B. Kang and C. G. Park, Strain-induced precipitation of NbC in Nb and Nb–Ti microalloyed HSLA steels, Scripta Mater., Vol 46(2), 2002, 163–168.
- [11]. A Ghosh, B. Mishra B.S. Das and S. Chatterjee, An ultra-low carbon Cu bearing steel: influence of thermomechanical processing and aging heat treatment on structure and properties, Mater. Sci. Eng.A, Vol. 374 (1–2), 2004, 43–55.
- a. Ghosh, B. Mishra, S. Das and S. Chatterjee, Structure and properties of a low carbon Cu bearing high strength steel, Materials Science and Engineering: A, Vol. 396, Issues 1–2, 15 April 2005, Pages 320–332

- [12]. Microalloying 2007, Proceedings of International Conference on Microalloyed Steels: Emerging Technologies and Applications, Kolkata, India, 2007
- [13]. Yu. Z. Babaskin and S. Y. Shipitsyn, Microalloying of Structural Steel with Nitride-Forming Elements, Steel in Translation, Allerton Press Inc, vol. 39(12), 2009, 1119-1121.
- [14]. A.P. A. Cunha, R.L. Villas Boas, S.T. Fonseca and P.R. Mei, Effect of Microalloying on Structure and Properties of Hot Rolled 0.5 %C Steel, Journal of Metallurgical Engineering (ME), vol. 2(2), 2013, 55-60.
- [15]. S. Panwar, D. B. Goel, O.P. Pandey and K S Prasad, Effect of microalloying on aging of a Cu-bearing HSLA-100 (GPT) steel, Bulletin of Materials Science, vol. 29(3), 2006, 281-292.
- [16]. S. Panwar, D. B. Goel, O.P. Pandey, Effect of cold work and aging on mechanical properties of a copper bearing microalloyed HSLA-100 (GPT) steel, Bull. Mater. Sci., vol. 30(2), 2007, 73-79.
- [17]. C. M. Spinelli and L. Prandi, High Grade Steel Pipeline for Long Distance Projects at Intermediate Pressure, 7th Pipeline Technology Conference, Hannover Congress Centrum, Hannover, Germany, March 2012.
- [18]. D. G. Stalheim and G Muralidharan, The Role of Continuous Cooling Transformation Diagrams in Material Design for High Strength Oil and Gas Transmission Pipeline Steels, Proceedings of IPC, IPC2006-10251, 2006, 231-238.
- [19]. N. S. Mourino, Crystallographically controlled mechanical anisotropy of pipeline steel, PhD Thesis, Ghent University, 2010.
- [20]. S. Vervynckt, Control of the Non recrystallization Temperature in High Strength Low Alloy (HSLA) Steels, PhD Thesis, Ghent University, 2010.
- [21]. S. Hertele, Coupled Experimental-Numerical Framework for the Assessment of Strain Capacity of Flawed Girth Welds in Pipelines, PhD Thesis, Ghent University, 2012.
- [22]. M. T. Miglin, J. P. Hirsh and A. R. Rosenfield, Metall. Trans. A, vol. 14A, 1983, 2055-61.
- [23]. R.J. Jesseman and G.J. Murphy, Mechanical properties and precipitation hardening response in ASTM A710 Grade A and A736 Alloy Steel Plates, Journal of Heat Treating, vol. 3(3), 1984, 228-236.
- [24]. G.E. Hicho, C.H. Brady, L.C. Smith and R.J. Fields, Effects of heat treatment on the mechanical properties and microstructures of four different heats of a precipitation hardening HSLA steel, Journal of Heat Treating, vol.5(1), 1987, 7-19.
- [25]. G.R. Speich and T.M. Scoonover, Continuous-Cooling-Transformation behavior and strength of HSLA-80 (A710) steel plates, in Processing, Microstructure and Properties of HSLA Steels, A.J. DeArdo, ed., TMS, Warrendale, PA, 1988, 263-286.
- [26]. S. Panwar, D. B. Goel, O. P. Pandey and K. S. Prasad, Aging of a copper bearing HSLA-100 steel, Bulletin of Materials Science, vol. 26(4), June 2003, 441-447.

MEASUREMENT OF AIR PRESSURE ON AUTOMOBILE

Ravi Dutt Sharma¹, Venkatsubramanian K²

¹School of Electronics Engineering (SENSE), VIT University
Vandalur, Kalambakkam Road, Chennai Tamil Nadu, (India)

²Assistant Professor School of Electronics Engineering (SENSE), VIT University
Vandalur, Kalambakkam Road, Chennai Tamil Nadu, (India)

ABSTRACT

Speed limit of a vehicle is decided depending upon the condition of road, traffic, government regulation and other real world constraints, one of them being the air pressure on the vehicle when it is moving on the road. Technically speaking it depends upon the drag coefficient of the vehicle being determined on the design of the car. Instead of using the traditional CAD design and testing tools or the numerical based approach here the below given system employs the technique being solely used for race car design testing or the Aeroplane test. This project employs a no of sensors to gather the data and LABview tool to analyse that and show the pressure on various zones of the vehicle.

Keywords: Labview, testing, Air pressure, vehicle Design, Drag coefficient

I. INTRODUCTION

Everyone today is in hurry to reach his destination as swift as possible, their delivery being made as soon as possible. Fuel is also an important factor to be considered which depends on the drag coefficient of the subject under study. Drag coefficient as per Wikipedia is a dimensionless quantity which is used to measure the resistance offered by an automobile travelling at high speed. It is because of two things one because of skin called as skin friction drag and second because of shape called as to be form drag. Mathematically

$$C_d = \frac{2 F}{\rho v^2 A}$$

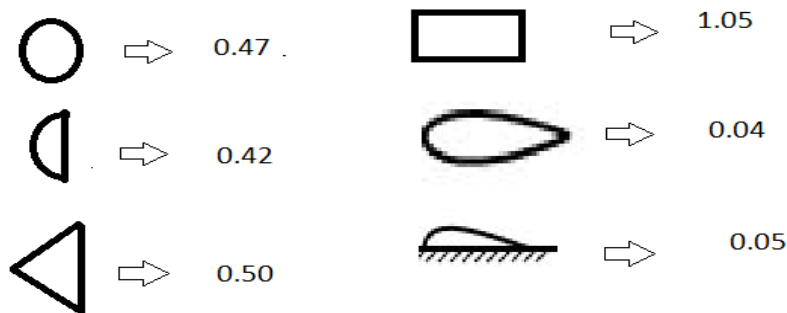
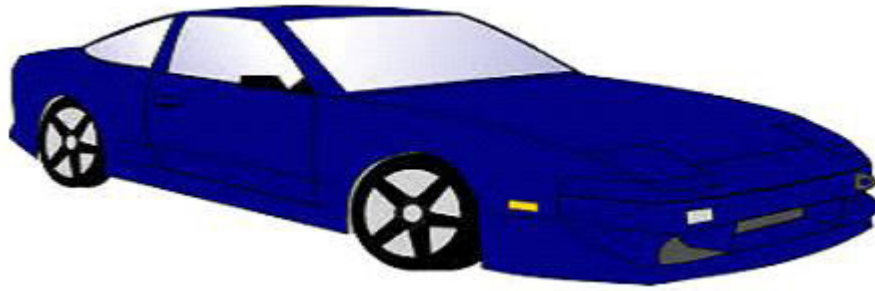


Fig.1 typical Values of Drag Coefficient of Various Shapes

Typical car designs are as depicted in the images below

Angular A and angular C pillar



Curved A and curved C pillar

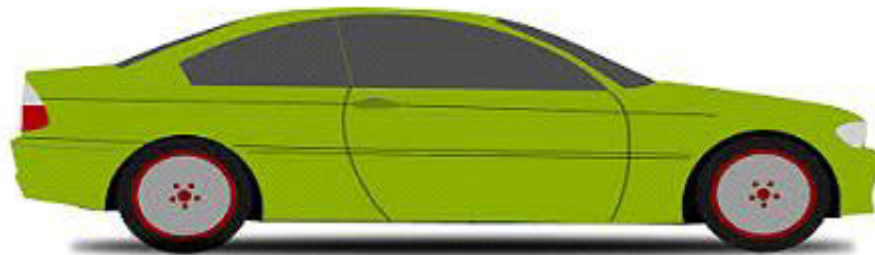


Fig. 2 Typical Car Designs

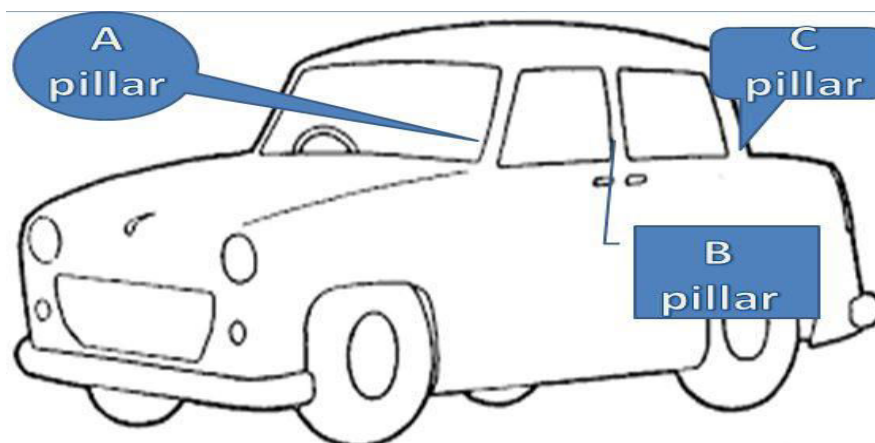


Fig. 3 Car Depicting Body Pillar of the Car

When air hits the automobile from the front end it has two effects one is reduced speed, causing discomfort in driving and higher fuel consumption, the other being lower grip of the vehicle on road as tries to lift it against gravity. For a heavy automobile such as truck the later problem is seldom observed but for light commercial vehicle and personal cars it a major issue of concern. Also at the time of car turning at curved roads and flyovers the air tries to drag the unstable vehicle to the edge and causing catastrophic situations. Hence all these constraints must be kept in mind while vehicle design.

Along with all these necessities there are some more such as safety of the passengers, look of the vehicle (attraction is a major force in case of personal automobile sales) and last but never the least is the cost of the subject the more time and money is spend in testing the costlier the vehicle get. To achieve this entire goal this paper discusses various tools and techniques a few of which worth mentioning are numerical based approach and CAD based analysis

1. Numerical based Approach

It uses the power of mathematics to check for the automobile design testing. The subject under consideration of our work is a Car model.

Any car design typically can be divided on the bases of pillar into three. A, B, C pillars which are as depicted into the picture just before.

A pillar and C pillar are the aerodynamically most important part of the car that causes the car to be unstable, reduced speed and lesser secure. In this approach without making the actual model everything is drawn on paper and is evaluated by making a lot of assumptions.

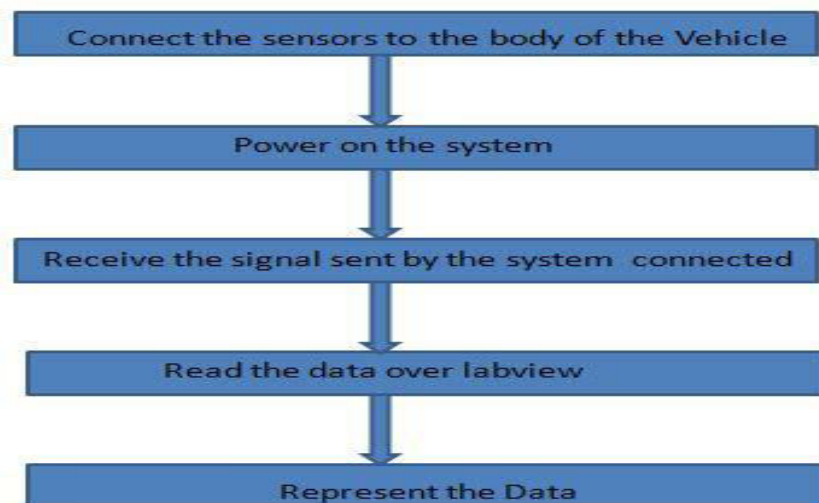
2. Computer based Design tools (CAD)

CAD tools have made our life simple by doing various calculations in background and making the response faster, reliable and represent able format. For these tools there is complex algorithm to show the outputs for the design being generated in a particular environment loaded with all design constraints for making it to appear as to be realtime.

But the problem with all these approaches is that they are all based on certain assumption and approximation. No matter how close to the real life they try to get the always lends up in a few or more assumption or costly setups.

II. METHODOLOGY/ ALGORITHM

This system is very generic in usage and is capable to be used for any vehicle under test as per the following algorithm



First connect the hardware being discussed shortly onto the surface of the vehicle. The system is then turned on and the data is now being transmitted by various sensors one by one on time sharing basis. The data being received is saved into a file format acceptable to the labview i.e. labview compatible. The data is then being represented using GUI feature of LABview.

III. CIRCUIT DIAGRAM

The circuit of the subject can be divided into two parts transmitter and receiver circuit. The transmitter is located at the vehicle site and the receiver being at a remote place.



Fig. 5 MPL 500



Fig. 6 Sensor Calibration

3.1 Transmitter Circuit

The system under the consideration is to be placed at a far place from the place where it is to be analysed so we have taken a device for remote space called as zigbee configured as to be router. To take the sensor data from the body of the automobile we have take a series of sensors from various manufacturers like MPL 502, MPL 500, BMP180

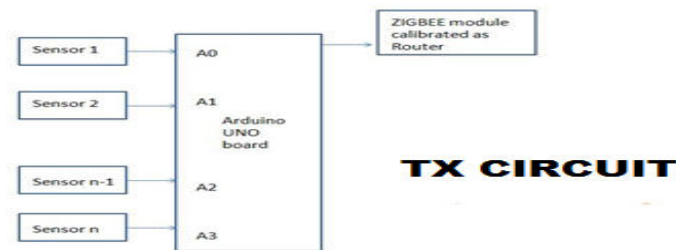


Fig. 4 Transmitter from Vehicle

An Arduino board is used to collect the analog data from these sensors and then send them one by one on TDM basis. Since the project uses a single zigbee transmitter module the TDM process for signal transmission and reception is used. Arduino UNO board is in built with a 4 channel 10 bit ADC so as to convert the data to digital format and then modulate the signal as per proper format. This system ported an RTOS on to the board so as to make the transmission to be very effective and to synchronize signal as per correct order

3.2 Receiver

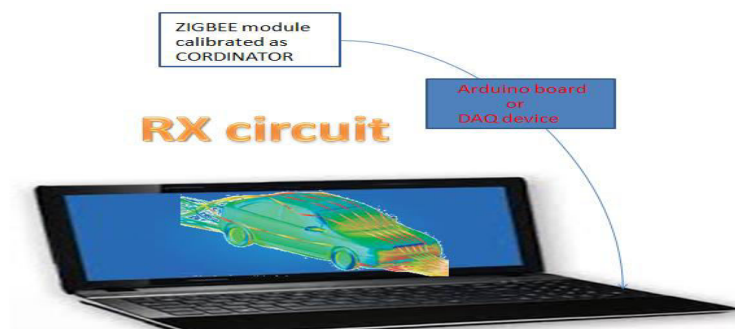


Fig. 5 Receiver of the Sensor Data at Distant Place

The signals that are sent from the TX circuit are received by the zigbee module configured as coordinator and the data is received serially.

This system is programmed to use an Arduino board as an interface b/w the LABview software installed in our system and the zigbee. After getting the data over LABview, data is manipulated and is displayed as some GUI.

IV. TOOL USED

The tool used for creating the module is LabVIEW by National Instrumentation ^[9] which is acronym for Laboratory Virtual Instrument Engineering Workbench. It is a visual programming tool for creating program. It is a very powerful and generic programming language which creates VI i.e. virtual instrument and can be called in other VI as sub VI for ease of programming.

Also the system uses XCTU for configuring the zigbee modules provided by xbee ltd. Arduino IDE is used to programme the Arduino UNO board.

V. RESULTS

The system was tested for two car designs and the various values of the sensor output are collected. A source with unknown levels of the wind pressure was taken and air was blown from the front end of the design. The sensors were pre calibrated using FRL system (a system capable of flowing air at non pressure ranging from 0 to 20 bars) and the typical sensor values were already recorded in a lookup table format and when unknown pressure was blown these values were matched and displayed. We have used 3 levels of air pressure on each design having 3 sensors over the subject under test. The results obtained are as

Table 1 Showing Pressures at Angular A and Curved C pillar Car (angle of A is 35*)

Pressure level	Pressure observed at in Bar		
	Sensor 1	Sensor 2	Sensor 3
1	1.5	1.3	1.01
2	1.7	1.4	1.01
3	1.9	1.5	1



Fig. 6 Sensor Value Plotted as Graphs

VI. CONCLUSIONS

Of various design of car that have been tried out results shows that angular A and curved C pillar design is best suited for the high speed application as they provide better stability and a reduced value of drag coefficient along with more comfort. As previously talked about, these various configurations causes the air flow dynamics misbalance as per the laws of physics under the car and opposite to the direction of it making it difficult to drive and less fuel economic. For an effective car design we must make the body streamlined as it makes the pressure of wind to be distributed in a balanced manner and avoiding it to get dislodge from the road.

An alert system can also be designed on this project so as to give warning to the driver if he is driving in improper manner or in hazardous conditions as to avoid loss of property and human life.

VII. SCOPE OF WORK

Since this project is only for college project here only 3 sensors have been incorporated but if provided with proper funding and professional excellence system which is having an array of sensors to read the data over various parts of the vehicle can be developed. These could be used to generate a point to point mapping of all the points of a car at their respective pressure levels. This is a very generic design circuit capable of implementation at various environments and for any designs.

This project as is clearly depicted is free from any errors because of assumption and is cost effective as the sensors and other hardware requirement are cheap in cost. This system can also be used to decide the speed limits of an automobile and at various road conditions.

VIII. ACKNOWLEDGMENT

My primary obligation is to authorities of VIT University (VITCC) who provided me the platform and opportunity to complete my project.

REFERENCES

- [1] Rizal E. M. Nasir,, FirdausMohamad“Aerodynamics of ARTeC’s PEC 2011 EMO-C Car ” in Procedia Engineering 41 (2012)
- [2] S. Diasinos, A. Gatto“Experimental investigation into wing span and angle-of-attack effects on sub-scale race car wing/wheel interaction aerodynamics” in Procedia Technology 4(2012) page 256 Elsevier
- [3] M. Tsubokura , S.Y. Cheng “Aerodynamic stability of road vehicles in dynamic pitching motion ” in Journal of Wind Engineering and Industrial Aerodynamicsissue 2 (2013)
- [4] Digi website for zigbee[Online] Available: <http://www.digi.com/>
- [5] Arduino website [Online] Available: <http://www.arduino.com/>
- [6] The IEEE website. [Online]. Available: <http://www.ieee.org/>
- [7] National Instrumentation.[Online] Available:<http://www.ni.com/>
- [8] Wikipedia website.[Online] Available: <http://www.wikipedia.org/>
- [9] *Google website* [Online] Available: <http://www.google.com/>

DETERMINATION OF EFFECTIVE ATOMIC NUMBER AND EFFECTIVE ELECTRON DENSITY OF WROUGHT ALUMINUM ALLOY 7017 FOR DIFFERENT PHOTON ENERGIES

A. S. Madhusudhan Rao¹, Abebe Getachew²

^{1,2}Assistant Professor, Dept of Physics, Hawassa University, Hawassa, (Ethiopia)

ABSTRACT

The effective atomic number (Z_{eff}) and effective electron density (N_{eff}) of wrought aluminum alloy 7017 has been estimated by determining the mass attenuation coefficient (μ_m), experimentally using narrow collimated beam transmission method with radioactive point sources of different γ -energies [(0.0595 MeV), (0.662 MeV), (1.173 MeV & 1.332 MeV)]. The transmitted γ -photons were detected and recorded by a NaI(Tl) scintillation detector with resolution of 8.5% for 661.16 KeV of ¹³⁷Cs. The linear attenuation coefficient (μ_l), total atomic cross section (σ_t), total electron cross section (σ_e) and photon mean free path (λ) for different γ -energies have been reported. The experimental results determined were compared with the theoretical values obtained using X-COM and semi empirical approach based on mixture rule for all photon energies. The experimental values are in good agreement with theoretical values.

Keywords: Mass Attenuation Coefficient, Linear Attenuation Coefficient, Effective Atomic Number, Effective Electron Density.

I. INTRODUCTION

The study of absorption of gamma radiation in shielding material is an important subject in the field of radiation physics. It is potentially useful in the development of semi-empirical formulations of high accuracy [1]. The interaction of high energy photons with matter is important in radiation medicine, biology, nuclear engineering and space technology. The study of parameters such as mass attenuation coefficient (μ_m), linear attenuation coefficient (μ_l), total atomic cross-section (σ_t), electronic cross-section (σ_e), effective atomic number (Z_{eff}), electron density (N_{eff}), mean free-path (λ) are important parameters in understanding the physical properties of composite materials. They are very important in many applied fields like nuclear diagnostics, radiation protection, nuclear medicine and radiation dosimetry.

Mass attenuation coefficient is a measurement of how strongly a substance absorbs or scatters radiation at a given wavelength, per unit mass. Mass attenuation coefficient can be used to derive other photon interaction parameters. Linear attenuation coefficient (μ_l) describes the fraction of a beam of X-rays or γ - rays that is absorbed or scattered per unit thickness of the absorber.

In 1982 Hubbell published tables of mass attenuation coefficients and the mass energy absorption coefficients for 40 elements and 45 mixtures and compounds over an energy range of 1 keV to 20 MeV. These tables,

although widely used, can now be replaced by the Hubbell and Seltzer tabulation for elements ($Z=1$ to 92) and 48 additional substances of dosimetric interest [1]. Berger and Hubbell developed the theoretical tables and computer program (XCOM) for calculating attenuation coefficients for elements, compounds and mixtures for photon energies from 1keV to 100 GeV[2, 3]. Recently, this well-known and much used program was modified to the Windows platform by Gerward et al. [4], and the Windows version is being called WinXCom. The scattering and absorption of gamma radiations are related to the density and atomic number of each element. In composite material like an alloy, it is related to density and effective atomic number. The knowledge of mass attenuation coefficients of alloys is of prime importance in the determination of effective atomic number. A single number therefore, cannot represent the atomic number uniquely across the entire energy range, since the partial interaction cross-sections depend on different element numbers [5]. The parameter “effective atomic number” has a physical meaning and allows many characteristics of material to be visualized with this number. The effective atomic number (Z_{eff}) of composite material is defined as the ratio of total atomic cross-section, to the total electronic cross-section [6, 7]. Attenuation coefficient and effective atomic number for many materials were reported [1-16]. In the present work, the mass attenuation coefficients and other photon interaction parameters of wrought aluminum alloy 7017 at [(0.0595 MeV), (0.662 MeV), (1.173 MeV & 1.332 MeV)] gamma energies are determined and are compared with the values obtained using semi empirical relations based on mixture rule and also with the values obtained from XCOM.

II. EXPERIMENTAL METHOD

Transmission experiments has been carried out with narrow beam good geometry setup (Gamma ray densitometer) shown in Fig.1. The setup with the source vault, collimators and the lead vault housing, the detector has been used for measuring the incident and transmitted intensities to determine the attenuation coefficient. The gamma rays are well collimated using lead collimators of cylindrical shape and a circular aperture of 6 mm diameter along the axis of the source and the detector. The signal is detected by NaI (TI) scintillation detector of 3×3 inch crystal under a high bias voltage of 1000 volts. The detector was shielded with a lead housing to reduce the radiation coming directly from the source scattered from the surroundings. The attenuation measurements were made with multichannel analyzer. The weak detector pulse is fed to the preamplifier which then enters the linear amplifier. The linear amplifier has two main functions of shaping the pulse and amplitude gain. The multi-channel analyzer (MCA) has been designed to work in conjunction with this setup. The amplified pulse is then fed to the MCA, which converts the analog signal into a digital signal using an analog to digital converter (ADC). Here, software installed in the MCA, is used to control the functions and other settings including the analysis of the spectrum. The energy and the efficiency of the system were calibrated using a certified standard source.

The alloy studied in the present work has been prepared by ingot metallurgy route. The alloy was melted in the air, in the induction furnace and cast iron moulds were used to obtain ingots. These ingots were subsequently homogenized and hot rolled to obtain 12 mm – 15 mm thick plates. The dimensions of the samples were measured with a screw gauge upto an accuracy of ± 0.01 mm. The alloy plates were precipitation strengthened by heat treatment, aging.

Alloy 7017 has chemical composition of 92.08% Al, 5.17% Zn, 2.26% Mg, 0.13% Zr, 0.28% Mn, 0.04% Fe and 0.04% Si by weight. The sample was shaped into a cuboid for measuring the attenuation. The sample was placed

between the source and the detector. The distance between the radioactive point source with sample and the sample to detector was 8 cm and 6 cm, respectively. The sample was irradiated with [(0.0595 MeV), (0.662 MeV), (1.173 MeV & 1.332 MeV)] photons emitted by 50 mCi Am-241, 100 mCi Cs-137 and 10 mCi Co-60 radioactive point sources respectively. I_0 and I the intensities before and after attenuation were measured by a high resolution detector. The measurements on sample were carried out five times at each energy value. In every case the photo-peak had Gaussian distribution. The peak areas have been estimated from the spectrum obtained for each measurement. Each spectrum was recorded for 30 minutes to record an adequate number of counts under the photo peak.



Fig. 1 The Experimental Setup

III. THEORY

The relations used in the present work are summarized in this section. Mass attenuation coefficients for the different materials and energies are determined by performing transmission experiments. This process is described by the following equation:

$$I = I_0 \exp(-\mu_m t) \quad (1)$$

Where I_0 and I are un-attenuated and attenuated photon intensities

$\mu_m = \mu/\rho$ (cm^2/g) is the mass attenuation coefficient

t (g/cm^2) is sample mass thickness (the mass per unit area)

The total mass attenuation coefficient μ_m for any chemical compound or mixture of elements is given by mixture rule [6]:

$$\mu_m = \sum_i w_i (\mu_m)_i \quad (2)$$

Where w_i is the weight fraction

$(\mu_m)_i$ is the mass attenuation coefficient of i th element

For a material composed of multi elements the fraction by weight is given by

$$w_i = \frac{n_i A_i}{\sum_i n_i A_i} \quad (3)$$

Where A_i is the atomic weight of the i^{th} element and n_i is the number of formula units.

The total atomic cross-section (σ_t) for materials can be obtained from the measured values of μ_m using the following relation

$$\sigma_t = \frac{\mu_m N}{N_A} \quad (4)$$

Where $N = \sum_i n_i A_i$ is atomic mass of materials (5)

N_A is the Avagadro's number.

Total electronic cross-section (σ_e) for the element is expressed by the following equation

$$\sigma_e = \frac{1}{N_A} \sum \frac{f_i N_i}{Z_i} (\mu_m)_i = \frac{\sigma_t}{Z_{eff}} \quad (6)$$

Where f_i denotes the fractional abundance of the element i with respect to the number of atoms such that $f_1+f_2+f_3+f_4+\dots+f_i=1$

Z_i is the atomic number of i^{th} element

The total atomic cross-section (σ_t) and total electronic cross-section (σ_e) are related to the effective atomic number (Z_{eff}) of the material through the following relation

$$Z_{eff} = \frac{\sigma_t}{\sigma_e} \quad (7)$$

Effective electron number or electron density (N_{eff}) (number of electrons per unit mass) can be calculated using the following relation:

$$N_{eff} = \frac{N_A}{N} Z_{eff} \sum n_i = \frac{\mu_m}{\sigma_e} \quad (8)$$

The average distance between two successive interactions, called the photon mean free path (λ), is given by

$$\lambda = \frac{\int_0^\infty x \exp(-\mu x) dz}{\int_0^\infty \exp(-\mu x) dx} = \frac{1}{\mu_l} \quad (9)$$

Where (μ_l) is linear attenuation coefficient and x is the absorber thickness.

The uncertainty in the measured physical parameters depends on uncertainty in the furnace temperature and measurement of the mass attenuation coefficient, which has been estimated from errors in intensities I_0 , I and thickness (l) using the following relation

$$\Delta(\mu_m) = \frac{1}{\rho l} \left[\left(\frac{\Delta I_0}{I} \right)^2 + \left(\frac{\Delta I}{I} \right)^2 + \left(\ln \frac{I_0}{I} \right)^2 + \left(\frac{\Delta l}{l} \right)^2 \right]^{1/2} \quad (10)$$

where ΔI_0 , ΔI and Δl are the errors in the intensities I_0 , I and thickness l respectively. In this experiment, the intensities I_0 and I have been recorded for the same time and under the same experimental conditions. Estimated error in these measurements was around 1%.

Theoretical values for the mass attenuation coefficients can also be obtained by Win Xcom program [17]. This program is based on mixture rule to calculate the partial and total mass attenuation coefficients for all elements and mixtures at standard as well as selected energies.

IV. RESULTS AND DISCUSSION

The mass attenuation coefficients have been calculated at the photon energies [(0.0595 MeV), (0.662 MeV), (1.173 MeV & 1.332 MeV)] The values obtained experimentally are compared with theoretical values calculated by using semi-empirical relations (1, 2 and 3) of section-3 and with the values of X-Com and are found to be in good agreement, as seen in the Table 1. It is clear that mass attenuation coefficient depends on photon energy and chemical content. The mass attenuation coefficient of a material decreases because probability of absorption reduces with increasing incident photon energies which results in the increase in the transmission of photons through it. The total experimental uncertainty of mass attenuation coefficient values depend on the uncertainties of peak area evaluation, mass thickness measurements, experimental system, counting statistics, and efficiency errors and so on. Using the mass attenuation coefficient, the parameters linear attenuation coefficient (μ_l), total atomic cross-section (σ_t), electronic cross-section (σ_e), effective atomic number (Z_{eff}), electron density (N_{eff}), mean free-path (λ) for wrought aluminum alloy 7017 at different photon energies have been calculated and the results have been displayed in Fig's (2-5) as function of photon energies.

Although the dependence of σ_t and σ_e on the photon energy is dominant at low energies, it is negligible at high energies The Z_{eff} and the N_{eff} remains constant and are found to be independent of photon energy for a compound. The electron density is closely related to the effective atomic number and hence has the same qualitative energy dependence, as effective atomic number. Total photon cross-section and electron cross-section (σ_t and σ_e) decreases with the increase in photon energy. Lastly, the photon mean free path (λ) for a compound found to be increasing with the photon energy. This is due to the decrease in the probability of interaction of photons in the material with the increase in energy. The variation in mass attenuation coefficient is due to the influence of other alloying elements present in the alloy. The agreement between the calculated values from semi empirical relations, XCOM and experimental results is good. However the presence of alloying elements in wrought aluminum alloy create a different environment in aluminum matrix, this could bring a change in the binding forces, chemical surroundings and distortion in crystallinity. But these changes in the aluminum matrix induced by the alloying elements are not considered when the values of mass attenuation coefficients were computed by XCOM and empirical relations. But the influence of these effects, discussed above, reflects in experimental measurements.

Hence the experimental values for the mass attenuation coefficients of aluminum alloy slightly differ from the calculated values. Further, the difference might arise in the values of μ_m obtained from experiment and calculation due to experimental setup and it's counting efficiency errors. Measured values of other photon interaction parameters like atomic cross section and electronic cross section show almost similar behavior as that of mass attenuation coefficient. The linear attenuation coefficient (μ_l) is determined for this alloy by using μ_m of the alloy. From the Table-1 it is clear that the linear attenuation coefficient is inversely proportional to energy. This is because as energy increases, the transmitted photons increase and the absorbed photons decrease, and hence linear attenuation coefficient decreases. The linear attenuation coefficient is related to the mean free

path which is the distance between successive interactions and mean free path is the inverse of the linear attenuation coefficient.

Table-1

μ , μ_l , σ_t , σ_e , Z_{eff} , N_{eff} and λ values (comparison between experimental, theoretical and X-com) of 7017 alloy at different γ -energies

E[MeV]	0.0595			0.662			1.173			1.332		
Parameter	X-Com value	Empirical value	Expt. Value	X-Com value	Empirical value	Expt. Value	X-Com value	Empirical value	Expt. Value	X-Com value	Empirical value	Expt. Value
$\mu_m (10^{-3}) \text{ m}^2\text{kg}^{-1}$	366.3	366.305	364.03	74.4	74.6162	74.1	56.67	56.6722	56.1	53.12	53.1278	52.1
$\mu_l \text{ m}^{-1}$	1010.99	1011	1004.72	205.344	205.941	204.516	156.409	156.415	154.836	146.611	146.633	143.796
$\lambda(10^{-4}) \text{ m}$	9.89131	9.89117	9.95299	48.6988	48.5577	48.8959	63.9349	63.9324	64.5845	68.2076	68.1975	69.543
$\sigma_t (10^{-24}) \text{ barn/atom}$	8.14957	8.14969	8.09906	1.65528	1.66009	1.6486	1.26081	1.26086	1.24813	1.18183	1.18201	1.15914
$\sigma_e (10^{-25}) \text{ barn/atom}$	2.84565	2.84569	2.82801	0.57799	0.57967	0.57566	0.44025	0.44027	0.43582	0.41267	0.41273	0.40475
$Z_{\text{effective}}$	28.6387	28.6387	28.6387	28.6387	28.6387	28.6387	28.6387	28.6387	28.6387	28.6387	28.6387	28.6387
$N_{\text{eff}}(10^{24}) \text{ electron/g}$	1.28723	1.28723	1.28723	1.28723	1.28723	1.28723	1.28723	1.28723	1.28723	1.28723	1.28723	1.28723

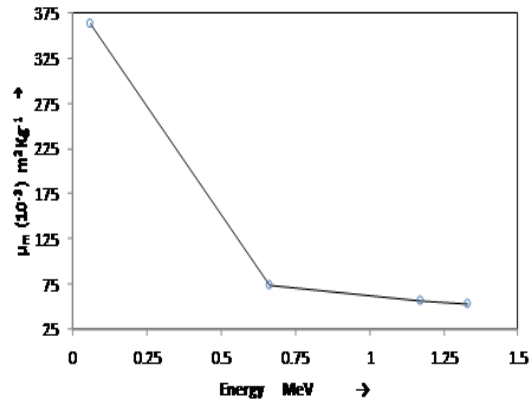


Fig.2 Mass attenuation coefficient vs Photon energy

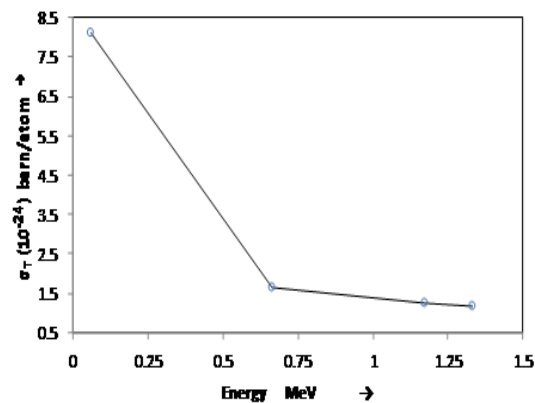


Fig.3 Total cross-section vs Photon energy

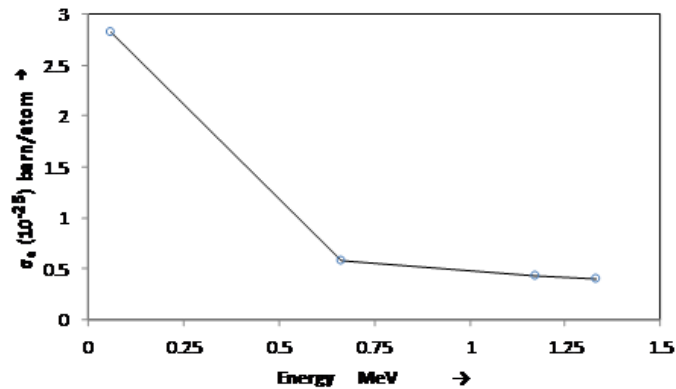


Fig.4 Electron Cross-Section vs Photon Energy

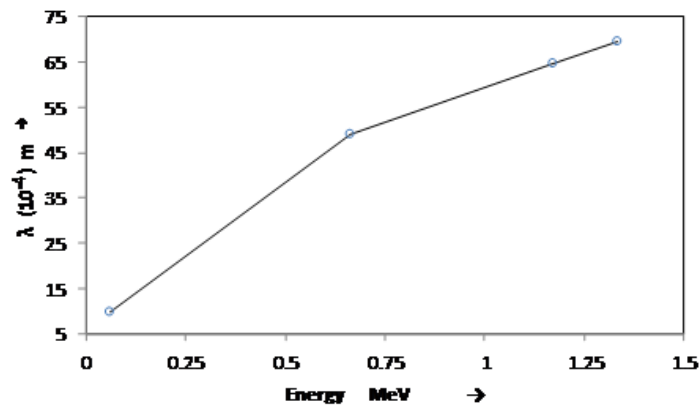


Fig.5 Mean Free Path vs Photon Energy

V. CONCLUSIONS

The present experimental study has been undertaken to determine the μ_m and related parameters for wrought aluminum alloy 7017. It can be concluded that the μ_m is a useful and sensitive physical quantity to determine the Z_{eff} and N_{eff} and other photon interaction parameters for alloys. In the interaction of photon with matter, μ_m values are dependent on the physical and chemical composition of the elements in the sample. The μ_m values of alloy decrease with increase in photon energy. Also, the variation of τ_t and τ_e with energy is identical to μ_m . The N_{eff} is closely related to the Z_{eff} and energy dependence of N_{eff} is the same as Z_{eff} . In the present study, it is evident that the μ_m , Z_{eff} and N_{eff} are useful parameters for alloys. The results of this study will be helpful in better understanding, of how the mass attenuation coefficients change with variation of the atomic and electronic number for different alloy compositions. To the best of our knowledge, experimental and theoretical investigations of the μ_m , τ_t , τ_e , Z_{eff} and N_{eff} for wrought aluminum alloy 7017 are not available in the literature. Moreover, the results of this work can stimulate both experimental and theoretical research for alloys.

REFERENCES

- [1]. Singh, K., Singh, H., Sharma, V., Nathuram, R., Khanna, A., Kumar, R., Bhatti, S.S. and Sahota, H.S., Gamma-Ray Attenuation Coefficients in Bismuth Borate Glasses, Nucl. Instru. and Meth. in Phys. Res. B, Vol.194, pp.1-6,2002.

- [2]. Singh, N., Singh, K.J., Singh, K. and Singh, H., Comparative Study of Lead Borate and Bismuth Lead Borate Glass Systems as Gamma-Radiation Shielding Materials, Nucl. Instru. and Meth. in Phys. Res. B, Vol.225, pp.305-309, 2004.
- [3]. Singh, S., Kumar, A., Singh, D., Singh, K. and Mudahar, G.S., Barium-Borate-Flyash Glasses:As Radiation Shielding Materials, Nucl. Instru. and Meth. in Phys. Res. B, Vol.266, pp.140-146, 2008.
- [4]. Gerward, L. Guilbert, N., Jensen, K.B. and Levring, H., WinXCom-A Program for Calculating X-Ray Attenuation Coefficients, Radiat. Phys. And Chem., Vol.71, pp.653-654, 2004.
- [5]. Singh, N., Singh, K.J., Singh, K. and Singh, H., Gamma-Ray Attenuation Studies of PbO-BaO-B₂O₃ Glass System, Radiat. Meas., Vol.41, pp.84-88, 2006.
- [6]. Cevik, U. and Baltas, H., Measurement of The Mass Attenuation Coefficients and Electron Densities for BiPbSrCaCuO Superconductor at Different Energies, Nucl. Instru. and Meth. in Phys. Res. B, Vol.256, pp.619-625, 2007.
- [7]. Singh, M.P., Sandhu, B.S. and Singh, B., Measurement of Effective Atomic Number of Composite Materials Using Scattering of γ -Rays, Nucl. Instru. and Meth. in Phys. Res. A, Vol.580, pp.50-53, 2007.
- [8]. Singh, K., Kaur, R., Vadana and Kumar, V., Study of Effective Atomic Numbers and Mass Attenuation Coefficients in Some Compounds, Radiat. Phys. Chem., Vol.47, No.4, pp.535-541, 1996.
- [9]. Kaewkhao, J., Tuscharoen, S., Limkitjaroenporn, P., Pokaipisit, A. and Chewpraditkul, W., Gamma-Rays Shielding Properties of Bi₂O₃- BaO-B₂O₃ Glasses System at 662 keV, Int. J. of Modern Phys. B, 2009, accepted manuscripted.
- [10]. Singh, K.J., Singh, N., Kaundal, R.S. and Singh, K., Gamma-Rays Shielding and Structural Properties of PbO-SiO₂ Glasses, Nucl. Instru. and Meth. in Phys. Res. B, Vol.266, pp.944-948, 2008.
- [11]. Baltas, H., Celik, S., Cevik, U., and Yanmaz, E., Measurement of Mass Attenuation Coefficients and Effective Atomic Numbers for MgB₂ Superconductor Using X-Ray Energies, Radiat. Meas., Vol.42, pp.55-60, 2007.
- [12]. Akkurt, I., Kilincarslan, S. and Basyigit, C., The Photon Attenuation Coefficients of Barite, Marble, and Limra, Ann. Nucl. Energy, Vol.34, pp.577-582, 2004.
- [13]. Singh, K. Singh, H., Sharma, G. Gerward, L., Khanna, A., Kumar, R., Nathuram, R. and Sahota, H.S., Gamma-Rays Shielding Properties of CaO-SrO-B₂O₃ Glasses, Radiat. Phys. And Chem., Vol.72, pp.225-228, 2005.
- [14]. Kaewkhao, J. et al., Determination of Effective Atomic Numbers and Effective Electron Densities of Cu/Zn Alloy, J. Quant. Spec. Raiat. Trans, Vol.109, pp.1260-1265, 2008.
- [15]. Creagh, D.C. and Hubbell, J.H., Problems Associated with The Measurement of X-Ray Attenuation Coefficients I. Silicon Report on The International Union of Crystallography X-Ray Attenuation Project, Acta. Cryst. A, Vol.43, pp.102-112, 1987.
- [16]. Creagh, D.C. and Hubbell, J.H., Problems Associated with The Measurement of X-Ray Attenuation Coefficients II. Carbon Report on The International Union of Crystallography X-Ray Attenuation Project, Acta. Cryst. A, Vol.46, pp.402-408, 1990.
- [17]. L. Gerward, N. Guilbert, K.B. Jensen, H. Levring, X-ray absorption in matter. Reengineering XCOM, Radiation Physics and Chemistry, 60 (2001) 23–24.

TELECOMMUNICATION FIBER OPTIC INFRASTRUCTURE WORLD- WIDE DEMAND: CASE STUDY

Dr. K. K. Saini¹, Mehak Saini²

¹Professor, ²Research Scholer, Dronacharya Engineering College Gurgaon, Gurgaon, (India)

ABSTRACT

Technology is often the mother of science. In the world of telecommunication fiber optic infrastructure has world- wide demand. They key requirement in today's world is wide bandwidth signal transmission with low delay. By the using optical fiber system we can provide enormous and unsurpassed transmission bandwidth with negligible latency. In this paper we will discuss the past, present and future aspects of fiber optics. We also discuss upcoming impact on next generation.

Index Terms- Bandwidth, Broadband, Fiber optics, Latency, Telecommunication.

I. INTRODUCTION

Fiber optics is the peer invention done by Narendra Singh Kapany and Charles K. Kao. Fibre optics's rapidly increasing consumer and commercial demand is the only driven force for the wide spread of it in whole world. By the help of this technology we can convey more data through a single optical fiber over a long distances. By the help of dispersion management we can improved the transmission capacity of the optical fiber.

Optic fiber system largely replaced the radio transmission system. It is widely used for telephony, internet traffic, LANs , cable T.V etc. In optical Fiber a single silica fiber can carry hundreds of thousands of telephone channels, utilizing only a small part of the theoretical capacity.

Day by day so many new technologies emerging such as CDMA , GSM, Wi-Max,etc. Within the last 30 years, the transmission capacity of optical fibers has been increased enormously. The rise in available transmission bandwidth per fiber is even significantly faster than e.g. the increase in storage capacity of electronic memory chips, or in the increase in computation power of microprocessors.

The transmission capacity of a fiber depends on the fiber length. The longer a fiber is, the more detrimental certain effects such intermodal or chromatic dispersion are, and the lower is the achievable transmission rate.

For short distances of a few hundred meters or less (e.g. within storage area networks), it is often more convenient to utilize multimode fibers, as these are cheaper to install (for example, due to their large core areas, they are easier to splice). Depending on the transmitter technology and fiber length, they achieve data rates between a few hundred Mbit/s and ≈ 10 Gbit/s.

Single-mode fibers are typically used for longer distances of a few kilometers or more. Currently used commercial telecom systems typically transmit 10 Gbit/s or 40 Gbit/s per data channel over distances of ten kilometers or more. The newest available systems (as of 2014) reach 100 Gbit/s, and future systems may use higher data rates per channel of e.g. 160 Gbit/s. The required total capacity is usually obtained by transmitting

many channels with slightly different wavelengths through fibers; this is called *wavelength division multiplexing* (WDM). Total data rates can be several terabits per second, sufficient for transmitting many millions of telephone channels simultaneously. Even this capacity does not reach by far the physical limit of an optical fiber. In addition, note that a fiber-optic cable can contain multiple fibers.

In conclusion, there should be no concern that technical limitations to fiber-optic data transmission could become severe in the foreseeable future. On the contrary, the fact that data transmission capacities can evolve faster than e.g. data storage and computational power, has inspired some people to predict that any transmission limitations will soon become obsolete, and large computation and storage facilities within high-capacity data networks will be extensively used, in a similar way as it has become common to use electrical power from many power stations within a large power grid. Such developments may be more severely limited by software and security issues than by the limitations of data transmission.

II. BASIC PRINCIPLES OF FIBER OPTIC

2.1 Communication

Fiber optic communication is a communication technology that uses light pulses to transfer information from one point to another through an optical fiber. The information transmitted is essentially digital information generated by telephone systems, cable television companies, and computer systems. An optical fiber is a dielectric cylindrical waveguide made from low-loss materials, usually silicon dioxide. The core of the waveguide has a refractive index a little higher than that of the outer medium (cladding), so that light pulses is guided along the axis of the fiber by total internal reflection [4]. Fiber optic communication systems consists of an optical transmitter to convert an electrical signal to an optical signal for transmission through the optical fiber, a cable containing several bundles of optical fibers, optical amplifiers to boost the power of the optical signal, and an optical receiver to reconvert the received optical signal back to the original transmitted electrical signal. Figure 1 gives a simplified description of a basic fiber optic communication system

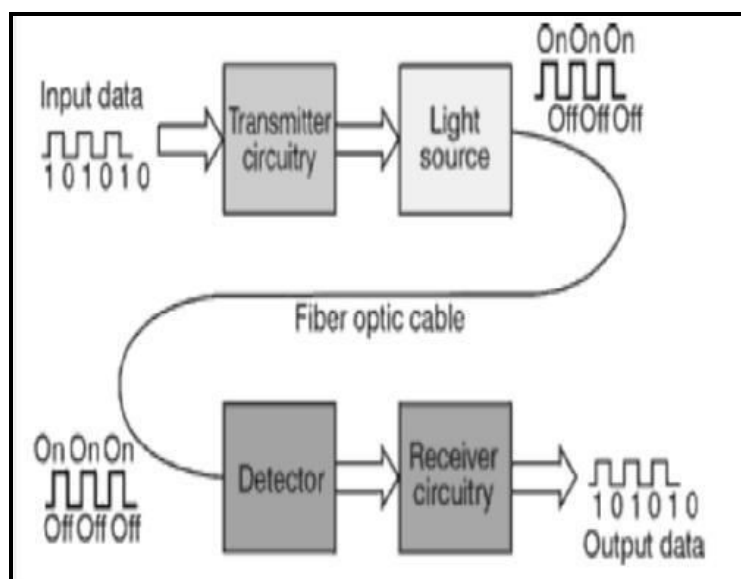


Fig.1. Basic Fiber Optic Communication System [5]

Optical fibers fall into two major categories, namely: step index optical fiber, which include single mode optical fiber and multimode optical fiber, and graded index optical fiber. Single mode step index optical fiber has a core diameter less than 10 micrometers and only allows one light path. Multimode step index optical fiber has a core

diameter greater than or equal to 50 micrometers and allows several light paths, this leads to modal dispersion. Graded index optical fibers have their core refractive index gradually decrease farther from the centre of the core, this increased refraction at the core centre slows the speed of some light rays, thereby allowing all the light rays to reach the receiver at almost the same time, thereby reducing dispersion. Figure 2 Gives a Description of the Various Optical Fiber Modes

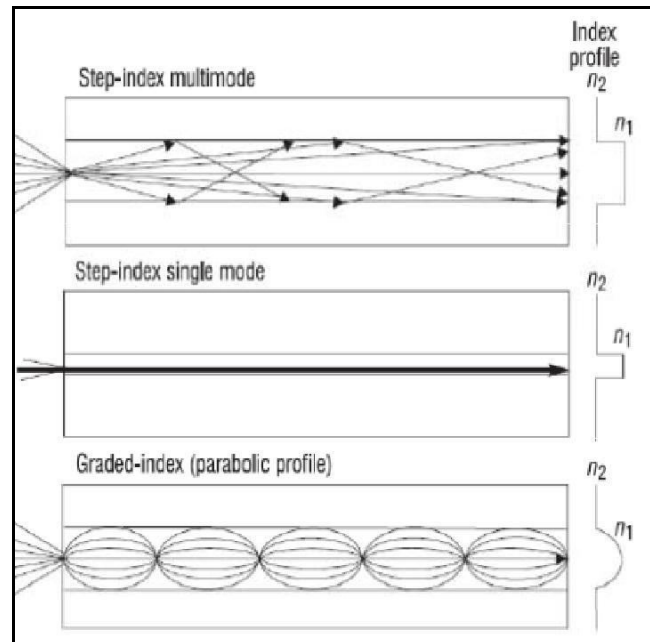


Fig.2. Optical Fiber Modes [6]

III. EVOLUTION OF FIBER OPTICS

3.1 Communication

Optical fiber was first developed in 1970 by Corning Glass Works. At the same time, GaAs semiconductor lasers were also developed for transmitting light through the fiber optic cables. The first generation fiber optic system was developed in 1975, it used GaAs semiconductor lasers, operated at a wavelength of $0.8 \mu\text{m}$, and bit rate of 45 Megabits/second with 10 Km repeater spacing.

In the early 1980's, the second generation of fiber optic communication was developed, it used InGaAsP semiconductor lasers and operated at a wavelength of $1.3 \mu\text{m}$. By 1987, these fiber optic systems were operating at bit rates of up to 1.7 Gigabits/second on single mode fiber with 50 Km repeater spacing.

The third generation of fiber optic communication operating at a wavelength of $1.55 \mu\text{m}$ was developed in 1990. These systems were operating at a bit rate of up to 2.5 Gigabits/second on a single longitudinal mode fiber with 100 Km repeater spacing.

The fourth generation of fiber optic systems made use of optical amplifiers as a replacement for repeaters, and utilized wavelength division multiplexing (WDM) to increase data rates. By 1996, transmission of over 11,300 Km at a data rate of 5 Gigabits/second had been demonstrated using submarine cables [7].

The fifth generation fiber optic communication systems use the Dense Wave Division Multiplexing (DWDM) to further increase data rates. Also, the concept of optical solitons, which are pulses that can preserve their shape by counteracting the negative effects of dispersion, is also being explored. Figure 3 shows the evolution of fiber optic communication.

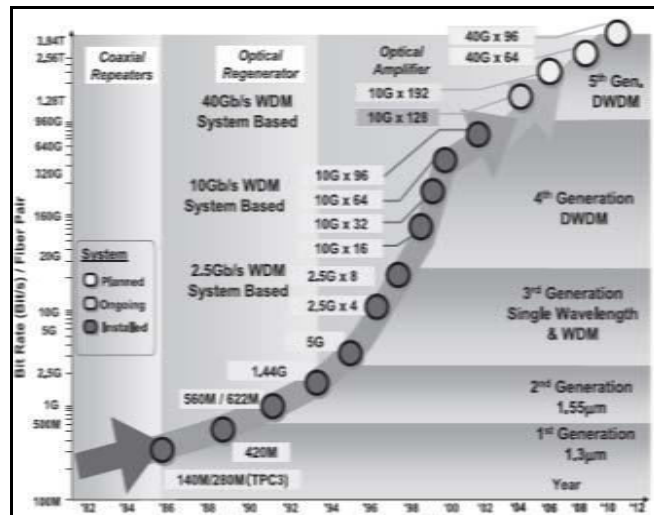


Fig.3. Generations of Fiber Optics Communication [8]

IV. FUTURE TRENDS IN FIBER OPTICS

4.1 Communication

Fiber optics communication is definitely the future of data communication. The evolution of fiber optic communication has been driven by advancement in technology and increased demand for fiber optic communication. It is expected to continue into the future, with the development of new and more advanced communication technology. Below are some of the envisioned future trends in fiber optic communication.

4.2 All Optical Communication Networks

An all fiber optic communication is envisioned which will be completely in the optical domain, giving rise to an all optical communication network. In such networks, all signals will be processed in the optical domain, without any form of electrical manipulation. Presently, processing and switching of signals take place in the electrical domain, optical signals must first be converted to electrical signal before they can be processed, and routed to their destination. After the processing and routing, the signals are then re-converted to optical signals, which are transmitted over long distances to their destination. This optical to electrical conversion, and vice versa, results in added latency on the network and thus is a limitation to achieving very high data rates.

Another benefit of all optical networks is that there will not be any need to replace the electronics when data rate increases, since all signal processing and routing occurs in the optical domain [9]. However, before this can become a reality, difficulties in optical routing, and wavelength switching has to be solved. Research is currently ongoing to find an effective solution to these difficulties.

4.3 Multi – Terabit Optical Networks

Dense Wave Division Multiplexing (DWDM) paves the way for multi-terabit transmission. The world-wide need for increased bandwidth availability has led to the interest in developing multi-terabit optical networks. Presently, four terabit networks using 40Gb/s data rate combined with 100 DWDM channels exists. Researchers are looking at achieving even higher bandwidth with 100Gb/s. With the continuous reduction in the cost of fiber optic components, the availability of much greater bandwidth in the future is possible.

4.4 Intelligent Optical Transmission Network

Presently, traditional optical networks are not able to adapt to the rapid growth of online data services due to the unpredictability of dynamic allocation of bandwidth, traditional optical networks rely mainly on manual configuration of network connectivity, which is time consuming, and unable to fully adapt to the demands of the modern network. Intelligent optical network is a future trend in optical network development [2], and will have the following applications: traffic engineering, dynamic resource route allocation, special control protocols for network management, scalable signaling capabilities, bandwidth on demand, wavelength rental, wavelength wholesale, differentiated services for a variety of Quality of Service levels, and so on. It will take some time before the intelligent optical network can be applied to all levels of the network, it will first be applied in long-haul networks, and gradually be applied to the network edge [10].

4.5 Ultra – Long Haul Optical Transmission

In the area of ultra-long haul optical transmission, the limitations imposed due to imperfections in the transmission medium are subject for research. Cancellation of dispersion effect has prompted researchers to study the potential benefits of soliton propagation. More understanding of the interactions between the electromagnetic light wave and the transmission medium is necessary to proceed towards an infrastructure with the most favorable conditions for a light pulse to propagate [11].

4.6 Improvements in Laser Technology

Another future trend will be the extension of present semiconductor lasers to a wider variety of lasing wavelengths [12]. Shorter wavelength lasers with very high output powers are of interest in some high density optical applications. Presently, laser sources which are spectrally shaped through chirp managing to compensate for chromatic dispersion are available. Chirp managing means that the laser is controlled such that it undergoes a sudden change in its wavelength when firing a pulse, such that the chromatic dispersion experienced by the pulse is reduced. There is need to develop instruments to be used to characterize such lasers. Also, single mode tunable lasers are of great importance for future coherent optical systems. These tunable lasers lase in a single longitudinal mode that can be tuned to a range of different frequencies.

4.7 Laser Neural Network Nodes

The laser neural network is an effective option for the realization of optical network nodes. A dedicated hardware configuration working in the optical domain and the use of ultra-fast photonic sections is expected to further improve the capacity and speed of telecommunication networks [12]. As optical networks become more complex in the future, the use of optical laser neural nodes can be an effective solution.

4.8 Polymer Optic Fibers

Polymer optical fibers offer many benefits when compared to other data communication solutions such as copper cables, wireless communication systems, and glass fiber. In comparison with glass optical fibers, polymer optical fibers provide an easy and less expensive processing of optical signals, and are more flexible for plug interconnections [13]. The use of polymer optical fibers as the transmission media for aircrafts is presently under research by different Research and Development groups due to its benefits. The German Aerospace Center have concluded that “the use of Polymer Optical Fibers multimedia fibers appears to be possible for future aircraft applications [14]. Also, in the future, polymer optical fibers will likely displace

copper cables for the last mile connection from the telecommunication company's last distribution box and the served end consumer [15]. The future Gigabit Polymer Optical Fiber standard will be based on Tomlinson-Harashima Precoding, Multilevel PAM Modulation, and Multilevel Coset Coding Modulation.

4.9 High – Altitude Platforms

Presently, optical inter satellite links and orbit-to-ground links exist [16], the latter suffering from unfavorable weather conditions [17]. Current research explores optical communication to and from high altitude platforms. High altitude platforms are airships situated above the clouds at heights of 16 to 25 Km, where the unfavorable atmospheric impact on a laser beam is less severe than directly above the ground [18]. As shown in figure 4, optical links between high-altitude platforms, satellites and ground stations are expected to serve as broadband back-haul communication channels, if a high-altitude platform functions as a data relay station.

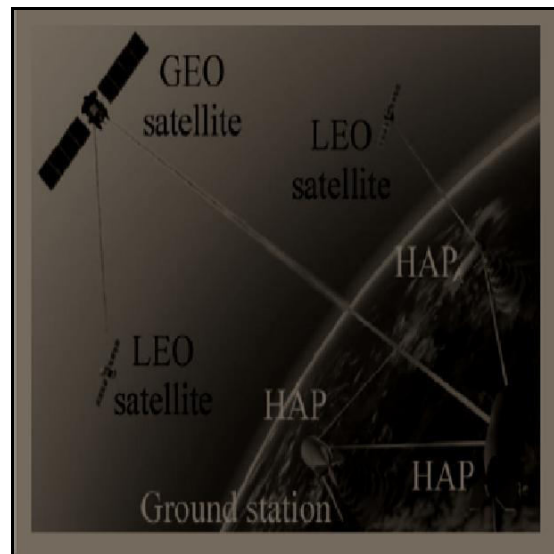


Fig.4. Laser Communication Scenarios from HAPs [4]

4.10 Improvements in Optical Transmitter/Receiver

4.10.1 Technology

In fiber optics communication, it is important to achieve high quality transmission even for optical signals with distorted waveform and low signal to noise ratio during transmission. Research is ongoing to develop optical transceivers adopting new and advanced modulation technology, with excellent chromatic dispersion and Optical Signal to Noise Ratio (OSNR) tolerance, which will be suitable for ultra-long haul communication systems. Also, better error correction codes, which are more efficient than the present BCH concatenated codes are envisioned to be available in the nearest future.

4.11 Improvement in Optical Amplification Technology

Erbium Doped Fiber Amplifier (EDFA) is one of the critical technologies used in optical fiber communication systems. In the future, better technologies to enhance EDFA performance will be developed. In order to increase the gain bandwidth of EDFA, better gain equalization technology for high accuracy optical amplification will be developed. Also, in order to achieve a higher output power, and a lower noise figure, high power pumping lasers that possess excellent optical amplification characteristics with outputs of more than +20dBm, and very low noise figure are envisioned to exist in the nearest future.

4.12 Advancement in Network Configuration of Optical

4.12.1 Submarine Systems

In order to improve the flexibility of network configuration in optical submarine communication systems, it is expected that the development of a technology for configuring the mesh network will be a step in the right direction. As shown in figure 5, while a ring network joins stations along a single ring, a mesh network connects stations directly. Presently, most large scale optical submarine systems adopt the ring configuration. By adopting the optical add/drop multiplexing technology that branches signals in the wavelength domain, it is possible to realize mesh network configuration that directly inter-connects the stations. Research is ongoing, and in the future such network configuration will be common.

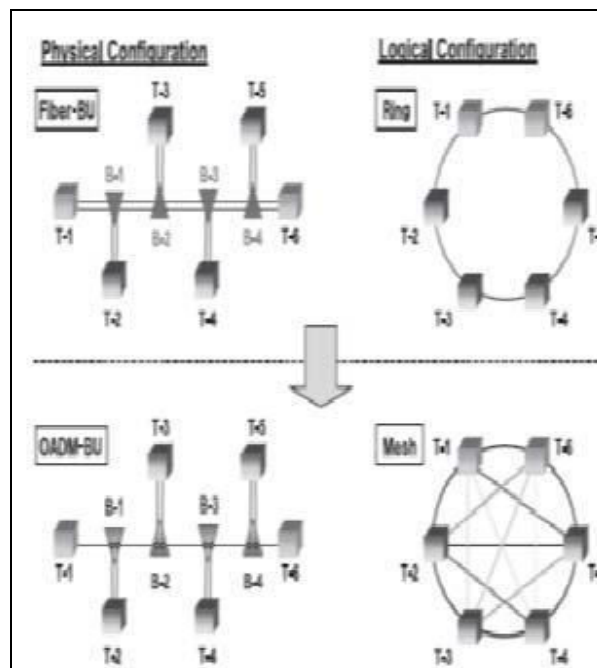


Fig.5. Optical Network Configurations [8]

4.13 Improvement in WDM Technology

Research is ongoing on how to extend the wavelength range over which wave division multiplexing systems can operate. Presently, the wavelength window (C band) ranges from 1.53-1.57 μm . Dry fiber which has a low loss window promises an extension of the range to 1.30 – 1.65 μm . Also, developments in optical filtering technology for wave division multiplexing are envisioned in the future.

4.14 Improvements in Glass Fiber Design and Component

4.14.1 Miniaturization

Presently, various impurities are added or removed from the glass fiber to change its light transmitting characteristics. The result is that the speed with which light passes along a glass fiber can be controlled, thus allowing for the production of customized glass fibers to meet the specific traffic engineering requirement of a given route. This trend is anticipated to continue in the future, in order to produce more reliable and effective glass fibers. Also, the miniaturization of optical fiber communication components is another trend that is most likely to continue in the future.

V. CONCLUSION

Optical Communication industry is an ever demanding one, the growth experienced by the industry has been enormous this past decade. Recently we have so many fields where optical communication is showing outstanding performance. There is still much work to be done to support the need for faster data rates, advanced switching techniques and more intelligent network architectures that can automatically change dynamically in response to traffic patterns and at the same time be cost efficient. The trend is expected to continue in the future as breakthroughs already attained in the laboratory will be extended to practical deployment thereby leading to a new generation in fiber optics communications.

REFERENCES

- [1] M. Noshada, A. Rostami, "FWM minimization in WDM optical communication systems using the asymmetrical dispersion managed fibers", International Journal for Light and Electron Optics, vol. 123, no. 9, pp. 758– 760, 2012.
- [2] X. Wang and K. Kitayama, "Analysis of beat noise in coherent and incoherent time-spreading OCDMA," IEEE/OSA Journal of Lightwave Technology ,vol. 22, no. 10, pp. 2226-2235, 2004.
- [3] T. H. Shake, "Confident performance of encoded optical CDMA", IEEE/OSA Journal of Lightwave Technology, vol. 23, pp. 1652- 1663, 2005.
- [4] Prachi Sharma et al, "A Review of the Development in the Field of Fiber Optic Communication Systems", International Journal of Emerging Technology and Advanced Engineering, Vol. 3, no. 5, pp. 113-119, 2013.
- [5] G. Keiser, op cit, p 51
- [6] Franz Fidler, Markus Knapek, Joachim Horwath, and Walter R.Leeb, "Optical Communications for High-Altitude Platforms", IEEE Journal of Selected Topics in Quantum Electronics, Vol. 16, no. 5, September/October 2010.
- [7] T. Otani, K. Goto, H. Abe, M. Tanaka, H. Yamamoto, and H.Wakabayashi, Electron. Lett.31, 380, 1995.
- [8] Ogata Takaaki, "Recent Status and Trends in Optical Submarine Cable Systems", NEC Technical Journal, Vol. 5 (1), pp. 4-7, 2010.
- [9] Colin Yao, "The Future of Fiber Optic Communication", available at: www.streetdirectory.com, 2013.
- [10] "Status of Optical Communication Technology and Future Trends", available at: www.qqread.net, 2013.
- [11] Djan Kloe, Henrie Van Den Boom, "Trends in Electro-optical Communication Systems, Perspectives on Radio Astronomy: Technologies for Large Antenna Arrays, Proceedings of the Conference held at the ASTRON Institute in Dwingeloo on 12- 14 April 1999. Edited by A. B. Smolders and M. P. Haarlem. Published by ASTRON. ISBN: 90-805434-2-X, 354 pages, 2000., p.2851999.
- [12] Pamela L. Derry, Luis Figueroa, Chi Shain Hong, "Semi-Conductor Lasers", 1991.
- [13] U.H.P. Fischer, M.Haupt and M.Janoic, "Optical Transmission Systems Using Polymeric Fibers", In Tech, available from: <http://www.intechopen.com/books>, 2011.
- [14] Cherian, S., Spangenberg, H. and Caspary, R., "Vistas and Challenges for Polymer Optical Fiber in Commercial Aircraft, Proceedings of the 19th POF Conference, 2010.
- [15] Koonen, A.M.J. et al, "POF Application in Home Systems and Local System", Proceedings of the 14th

POF Conference, pp. 165-168, 2005.

- [16] T. Jono, Y. Takayama, K. Shiratama, I. Mase, B. Demellenne, Z. Sodnik, A. Bird, M. Toyoshima, H. Kunimori, D. Giggenbach, N. Perlot, M. Knappek, and K. Arai, Overview of the inter-orbit and the orbit to-ground laser communication demonstration by OICETS, SPIE, vol. 6457, pp. 645702-1–645702-10, 2007.
- [17] COST297. HAPCOS, “High Altitude Platforms for Communications and Other Services”, Available Online at: <http://www.hapcos.org>, 2010.
- [18] L. C. Andrews and R. L. Phillips, Laser Beam Propagation through Random Media, 2nd ed. Bellingham, WA: SPIE, 2005.

COMPRESSIVE AND SPLIT TENSILE STRENGTHS OF POLYETHYLENE TEREPHTHALATE (PET) FIBRE REINFORCED RECYCLE AGGREGATE CONCRETE

N.Venkata Ramana¹, R.Harathi², Vaishali G Ghorpade³

¹Associate Professor, Civil Engineering Department, UBDT College of Engineering, Davangere,
Karnataka (State), (India)

²Assistant Executive Engineers, PABR sub division no:3, , HLC Division, I and CAD Department
Anantapuram, Andhra Pradesh (State), (India)

³Professor, Department of Civil Engineering, JNTUA College of Engineering Anantapur,
Andhra Pradesh (State), (India)

ABSTRACT

This paper presents the compressive and split tensile strength of PET fibre reinforced recycles aggregate concrete. The Natural Aggregate (NC) was replaced by recycle aggregate (RA) in the proportion of 25, 50, 75 and 100%. PET fibres are added to the Recycle Aggregate Concrete (RAC) by 1 and 2% volume. The results showed that as the % of RA and volume fraction of PET fibre content increases the strength was decreased. For obtained experimental results Regression Model (RM) was developed to predict the split tensile strength by knowing the compressive strength of concerned mix of concrete and the same is presented in this article.

Key Words:-RAC, PET Fibres, Compressive Strength, Cube, Split Tensile Strength, Cylinder, Regression Model

I. INTRODUCTION

For design grade of concrete the aggregate (coarse and fine) occupies about three fourth (3/4) of the volume of specimen and play a significant role in concrete properties such as fresh and harden concrete properties, dimensional stability and durability. Conventional concrete consists of sand as fine aggregate and gravel (granite in various sizes and shapes) as coarse aggregate. There is a growing interest in using waste materials as alternative aggregate materials. In this context Demolished Waste Material (DWM) of building or any structure (after completing of its lifespan) or during modernization, waste is generated. This can be utilized in the concrete as recycle aggregate (RA). Many research works has been carried out on Recycle aggregate concrete (RAC). Now days the plastic is also is a waste and this waste is using for many works as recycle products. Among the different type of plastics groups, Polyethylene Terephthalate (PET) is one of the major products using by the society in the form of various articles. In this connection a review is presenting below related to PET fibres and RAC. Marzouk et.al. [1] conducted the experimentation on concrete with plastic waste. The plastic material was used as sand substitution in the concrete. The results showed that the use of plastic bottle waste was effective and it attracts as low cost material. Siddique et.al.[2] investigated the effective utilization of

waste products (tires, plastic, glass etc) in concrete. The study showed that the use of waste product in concrete not only makes it economical but also helps in reducing disposal problem. Kou et.al.[3] reported that splitting tensile strength of PVC concrete. From their study it is noticed that as PVC content increases the strength was decreased. Akcaozoglu et.al. [4] investigated the use of shredded waste polyethylene using two types of binders. The authors found that the compressive strengths of mortar with PET aggregate is higher with combination of binders. Kandasamy and Mrugesan [5] reported the behavior of composite material consisting of cement based matrix with an ordered or random distribution of fibre of steel, nylon, polythene. The results showed that the addition of fibres increases the properties of concrete. BabooRai et.al.[6] reported the concrete properties produced with waste plastic with and without plasticizer. The study showed that reduction in workability and compressive strength with inclusion of plastic. But they also specified that with addition of Plasticizer the strengths were increased marginally. Bhogayata et.al.[7] presents a comparative study of compressive strength of concrete made by mixing of plastic bags as concrete constituent. The results showed that as increase of plastic the compaction factor and compressive strength decreases. JianzhuangXialet.al[8] has given a overview of study on recycle aggregate concrete. In this paper different properties of RAC and its behaviour was described. Xiao.J.Zh. et.al [9] has shown relationships between mechanical properties of RAC. From literature it is observed that there is a little work has been focused on PET fibres with combination of RA. So the authors had planned to evaluate compressive strength (CS) and split tensile strength (STS) of PET fibre recycle aggregate concrete and also to establish the relation between the two strengths. To find CS and STS of PET fibre reinforced recycle aggregate concrete, 45 cubes and 45 cylinders were cast and tested in the laboratory.

II. MATERIALS USED

- 1) **Cement:** Ordinary Portland cement–53 grade was used. The specific gravity of cement was found as 3.15 and it satisfies the requirements of IS: 12269–1987 specifications.
- 2) **Super plasticizer:** To impart the additional desired properties, a super plasticizer (Conplast SP-430) was used. The dosage of super plasticizer adopted in the investigation was 0.85% (by weight of cement).
- 3) **Sand:** Locally available sand collected from river bed was used as fine aggregate. The sand used was having fineness modulus 2.96 and confirmed to grading zone-III as per IS: 383-1970 specification.
- 4) **Coarse aggregates:** The crushed stone aggregates were collected from the local quarry. The coarse aggregates used in the experimentation were 20mm and down size aggregate and tested as per IS: 383-1970 and 2386-1963 (I, II and III) specifications. The specific gravity was observed as 2.65.
- 5) **Recycle aggregate concrete:** The Recycled coarse aggregate obtained by crushing demolished concrete mass and the same was used as recycled coarse aggregate in the present investigation. To obtain a reasonably good grading, 50% of the aggregate passing through 20 mm I.S. sieve and retained on 12.5mm I.S. Sieve and 50% of the aggregate passing through 12.5mm I.S. Sieve and retained on 10 mm I.S. Sieve is used. The specific gravity was found as 2.48.
- 6) **Water:** Ordinary potable water, free from organic content, turbidity and salts was used for mixing and for curing throughout the investigation.
- 7) **PET Fibres:** The waste PET fibres were obtained by cutting of unused drinking water bottles. The fibres were cut from steel wire cutter and it is labor oriented. The PET fibres were sieved and found that 10mm size are more in fiber content and the thickness was observed as 1mm. (Figure. 1)



Figure.1 PET fibres

III. CASTING AND CURING

Concrete was prepared by a design mix proportion of 1:1.90:3.09 with a W/C ratio of 0.45 which correspond to M20 grade of concrete. The entire mix was homogeneously mixed with calculated quantity of required materials. The standard cubes and cylinders were (cube size is 150 x 150 x 150mm and cylinder size is 150mm dia, 300mm height) cast and tested after 28 days of curing as per IS specifications. A total 15 mixes (45 cubes & 45 cylinders) were considered in the investigation and for each mix three cubes and three cylinders are tested. The average value of ultimate load and stress of three cube and cylinder specimens are presented in Table.1. In the table.1, RAC indicates recycle aggregate concrete, F1 and F2 indicates PET fibre volume fraction of 1 and 2% by volume of cast specimen and the number 0,25,50,75 and 100 indicates the % of replacement of granite aggregate with recycle aggregate. The RAC-0 considered as reference mix (M20) or Natural aggregate concrete (NAC), in this forthcoming sections, the other mixes were compared with reference mix or NAC.

IV. TEST RESULTS AND DISCUSSION

4.1 Compressive Strength

The compressive strength results are presented in Table.1. From this table it is observed that as % of RA content increases the compressive strength decreases. For 25 to 75% replacement of RA in conventional mix the strength decrement is about 2 to 14%. The reason may be the bond between recycle aggregate concrete and new cement mortar forms weak links, but it is vice versa for NA. The Compressive strength of RAC with fibres is in the range of 30 to 19 MPa. As the % fibre increase the compressive strength decreases. The design compressive strength of concrete is 20MPa, for PET fibre RAC this value touches at 2% of PET fibre and 75% RA. This indicated that, RAC with 1% fibre volume and upto 100% replacement of RA is effectively utilized, but the RAC with 2% fibre upto 75% replacement of RA is permitted for the designer/engineer incharge at site. The decrease in compressive strengths for RAC with PET fibres may be due to low bond strength between the surface of plastic waste and cement paste as well as the hydrophobic nature of plastic waste, which can inhibit cement hydration reaction by restricting water improvement and another reason may be particle size and shape between natural and plastic fibre. Frigione[10] was reported this type of trend for natural aggregate concrete with plastic waste. Venkata Ramana et al., [11] developed some regression models to predict the compressive strengths for 0,1 and 2% of PET fibres for recycle aggregate concrete.

4.2 Split Tensile Strength

The split tensile strength results are presented in Table.1. From the results it observed that as the % of RA content increases the tensile strength is decreased. The % of decrease is about 1 to 9% for 25 to 100% replacement of RA. Mukaiet.al[12] and Ravindrarahaj[13] reported the similar observations. They reported that for recycle aggregate concrete the split tensile strength is about 10 to 20% of conventional concrete.

The split tensile strength of RAC with PET fibres is decreasing as % of PET fibre volume increases. The percentage of decrement for 1% fibre is 5 to 17% and for 2% fibre 23 to 32% for RAC concrete when compared with conventional concrete. The decrement in strength may be due to interfacial transition zone, the smooth surface of PET fibres causes weaker bond between the plastic and additive material(cement paste).Kou et.al [14] reported the same trend results for concrete.

From through inspection of tested specimen the author noticed that the concrete cylinders with PET fibres did not split into two fractions after determination of tensile strength.The probable reason may be the PET fibres may act as bridge between the two split pieces.

Table.1: Compressive and Split Tensile Strengths

Sl.No.	Nomenclature	Average Ultimate compressive Load(KN)	Average Ultimate Compressive Strength (N/mm ²)	% of Decrease or increase of compressive strength	Average Split tensile Load(KN)	Average split tensile Strength (N/mm ²)	% of Decrease or increase of split tensile strength
1	RAC-0	750	33.33	-	240	3.39	-
2	RAC-25	723	32.13	-2.89	236	3.34	-1.47
3	RAC-50	696	30.93	-7.2	230	3.25	-4.12
4	RAC-75	673	29.19	-12.42	224	3.17	-6.48
5	RAC-100	645	28.6	-13.98	219	3.09	-8.85
6	RACF1-0	680	30.22	-9.33	226	3.19	-5.89
7	RACF1-25	647	28.75	-13.74	219	3.09	-8.85
8	RACF1-50	619	27.51	-17.46	215	3.04	-10.32
9	RACF1-75	596	26.54	-20.55	209	2.95	-12.97
10	RACF1-100	577	25.64	-23.07	200	2.83	-16.51
11	RACF2-0	506	22.48	-32.55	185	2.61	-23.00
12	RACF2-25	485	21.55	-35.34	180	2.55	-24.77
13	RACF2-50	467	20.75	-37.74	174	2.46	-27.43
14	RACF2-75	452	20.08	-39.97	170	2.40	-29.20
15	RACF2-100	436	19.37	-41.88	164	2.32	-31.56

4.3 Relation between Split Tensile Strength and Compressive Strength

The split tensile strength is often used to obtain the tensile strength of concrete, rather than by a direct tensile strength test, because the former is easier to perform. In practical applications, the tensile strength of concrete is often estimated from the compressive strength. The split tensile strength of the RAC with relation of

compressive strength was obtained by the previous investigators of Xiao et al. [15] as $f_t = 0.75(f_{ck})^{0.5}$. This relation was deduced for RAC without considering the PET fibre. In the ACI 318-M-11 code and Chinese code (GB 50010-2002). The relationship between split and compressive strength normal concrete expressed as

$$f_{sp} = 0.49 \sqrt{f_{ck}} \text{----- As per ACI code}$$

(Note: cylinder compressive strength = 0.76 compressive strength)

$$f_{sp} = 0.19(f_{ck})^{0.75} \text{----- As per GB code}$$

By using the above equations the results are presented in Table 2. From this table it is observed that the results under estimates for RAC concrete with and without fibres. To improve the above equations a regression analysis was performed to the obtained test results and the following regression equation is deduced with correlation coefficient R² is 0.996 and Standard Deviation (SD) is 0.022.

$$f_{sp} = 0.78 \sqrt{f_{ck}} - 1.12$$

Comparison between the test results and that predicted by proposed equation is presented in Table.3 and Figure.1 The ratio between EXP/RM is about 1.0 to 1.02. From this it noticed that the proposed equation has good agreement with the experimental results.

Table.2: Comparison of Experimental Split Tensile Strength with Different Codes

Sl.No	Nomenclature	EXP Split tensile strength	As per Xiao et.al	ACI	GB	EXP/Xiao	EXP/ACI	EXP/GB
1	RAC-0	3.39	2.34	2.83	2.64	1.45	1.20	1.29
2	RAC-25	3.34	2.29	2.78	2.56	1.46	1.20	1.30
3	RAC-50	3.25	2.23	2.73	2.59	1.46	1.19	1.30
4	RAC-75	3.17	2.15	2.65	2.39	1.47	1.20	1.33
5	RAC-100	3.09	2.13	2.62	2.35	1.45	1.18	1.31
6	RACF1-0	3.19	2.20	2.69	2.45	1.45	1.18	1.30
7	RACF1-25	3.09	2.13	2.63	2.36	1.45	1.18	1.31
8	RACF1-50	3.04	2.07	2.57	2.28	1.47	1.18	1.33
9	RACF1-75	2.95	2.02	2.52	2.22	1.46	1.17	1.33
10	RACF1-100	2.83	1.98	2.48	2.16	1.43	1.14	1.31
11	RACF2-0	2.61	1.82	2.32	1.96	1.44	1.12	1.33
12	RACF2-25	2.55	1.77	2.27	1.90	1.44	1.12	1.34
13	RACF2-50	2.46	1.72	2.23	1.85	1.43	1.10	1.33
14	RACF2-75	2.40	1.69	2.20	1.80	1.42	1.09	1.33
15	RACF2-100	2.32	1.65	2.16	1.75	1.41	1.08	1.32

Table 3: Regression Model Performance for Split Tensile Strength

Sl.No	Nomenclature	Experimental Split tensile strength	Regression Model	Exp Split tensile strength / Regression Model
1	RAC-0	3.39	3.38	1.00
2	RAC-25	3.34	3.30	1.01
3	RAC-50	3.25	3.21	1.01
4	RAC-75	3.17	3.09	1.02
5	RAC-100	3.09	3.05	1.01
6	RACF1-0	3.19	3.16	1.01
7	RACF1-25	3.09	3.06	1.01
8	RACF1-50	3.04	2.97	1.02
9	RACF1-75	2.95	2.89	1.02
10	RACF1-100	2.83	2.82	1.00
11	RACF2-0	2.61	2.57	1.01
12	RACF2-25	2.55	2.50	1.02
13	RACF2-50	2.46	2.43	1.01
14	RACF2-75	2.40	2.37	1.01
15	RACF2-100	2.32	2.30	1.01

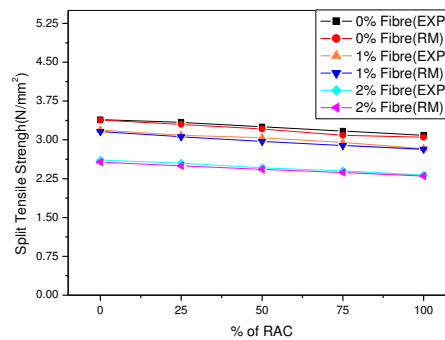


Fig.2: Performance of Regression Model

V. CONCLUSIONS

The following conclusions are drawn from the present experimental work.

1. The compressive and split tensile strengths are decreases as the RA content increase in the conventional concrete mix.
2. The compressive and split tensile strengths decreased about 2 to 14% and 1 to 8% with RA content of 25 to 100% respectively
3. As PET fibre volume increases in the RAC the compressive and split tensile strengths are decreased.
4. The PET fibre volume with 1% can be used effectively without change in design mix.
5. The Maximum permissible limit for recycle aggregate content with 2% fibre volume is 75%.

6. For RAC with 1% PET fibre volume the compressive and split tensile strengths decreased about 9 to 23% and 6 to 17% with RA content of 0 to 100% respectively when compared with conventional concrete.

7. For RAC with 2% PET fibre volume the compressive and split tensile strengths decreased about 32 to 42% and 25 to 31% with RA content of 0 to 100% respectively when compared with conventional concrete.

REFERENCES

- [1] Marzouk O Y, Dheilily RM, Queneudec M, Valorization of post consumer waste plastic in cementitious concrete composites, *Waste Manage*, 27, pp310-318, 2007.
- [2] Siddique R, Khatib J, Kaur I, "Use of recycled plastic in concrete, A review waste management" 28, pp1835-1852, 2008.
- [3] Kou SC, Poon CS, "Properties of light weight aggregate concrete prepared with PVC granules derived from scraped PVC pipes", *Waste manage (Oxf)*, 29(2), pp621-628, 2009.
- [4] Akcaozoglu S, Atis CD, Akcaozoglu K, "An investigation on the use of shredded waste PET bottles as aggregate in light weight concrete", *Waste manage (Oxf)*, 32(2), pp258-290, 2010.
- [5] Kandasamy R and Murugesan R, "Fibre reinforced concrete using domestic waste plastic as fibres", *ARPN journal of Engineering and Applied Sciences*, 6(3), pp75-82, 2011.
- [6] Baboo Rai, Tabin Rushad S, Bhavesh KR, Duggal SK, "Study of waste plastic mix concrete with plasticizer", *ID* 4692, 72, pp1-5, 2012.
- [7] Bhogayata A, Shah K D, Vyas B A, Arora N K "Performance of concrete by using Non recyclable plastic wastes as concrete constituent", *International journal of Engineering Research and Technology (IJERT)*, 1(4), pp1-3, 2012.
- [8] Jianzhuang Xiao, Wengui Li, Yuhui Fan, Xio Huang, "An over view of study on recycle aggregate concrete in china (1996-2011)", *Construction and building materials*, 31, pp364-383, 2012.
- [9] Xiao J.Zh., J.B. Li. Ch Zhang, "On relationship between the mechanical properties of recycle aggregate concrete: An over view", *Materials and structures*, 39, pp655-664, 2006.
- [10] Frigione M, "Recycling of PET bottle as fine aggregate in concrete", *Waste Manage (Oxf)*, 30(6), pp1101-1106, 2010.
- [11] Venkata Ramana. N, R. Harathi, S. Narasimha Babu, S. Vinay Babu, "Regression", *International Journal of Engineering Research and Development*, Volume 8, Issue 5 PP. 11-16 (August 2013).
- [12] Mukai T, Kikuchi M, "Studies on utilization of recycled concrete for structural members (part 1 and part 2). Summaries of technical papers of annual meeting, *Arcchit Inst Jpn*, pp85-88, 1978.
- [13] Ravindrarajah RS, Tam TC (1985), Properties of concrete made with crushed concrete as coarse aggregate, *Maga Concrete Res*, 37(130), pp29-38, 1985.
- [14] Kou SC, Lee G, Poon CS, Lai WL, "Properties of light weight aggregate concrete prepared with PVC granules derived from scraped PVC pipes" *Waste Manage (Oxf)* 29(2), pp621-628, 2009.
- [15] Xiao JZ, Li JB, Zhang C, "On relationship between the technical properties of recycle aggregate concrete: an overview" *Material Struct*, 39(6): pp655-664, 2006

VEHICLE DETECTION AND COUNTING

Roopashree C¹, T.R Sateesh kumar²

¹PG Scholar, Signal Processing, ²Assistant Professor, ECE, Siddaganga Institute of Technology,
Tumkur, Karnataka, (India)

ABSTRACT

Video Surveillance is a very important aspect in computer vision because these systems do not disturb traffic during installation and they are easy to modify. Vehicle detection and counting is very important in traffic monitoring, military applications, toll collection etc. The input video clip is taken, frames are extracted and background is estimated. By this estimated background the next frames are subtracted to detect moving objects. In that moving objects vehicles are detected, classified and counted for traffic estimation. Experiments are carried out by taking the input video in varying environments. Experiments are implemented with Microsoft Visual studio 2010 C++ software with OpenCV.

Keywords: *Background Subtraction, Classification, Frames Extraction, Segmentation, Vehicle Counting.*

I. INTRODUCTION

Intelligent Transport System (ITS) is gaining very importance now a days, because everywhere we can find CCTV cameras which are used for security purpose and to keep track on the whereabouts on that region. Traffic monitoring is also very important because of increasing traffic accidents [1]. Therefore Vehicle detection and counting is very important in traffic congestion, keep tracking of vehicles and to control the traffic signal duration.

Automatic vehicle counting can also be used to allot the empty slots in parking systems by counting the number of vehicles entering and leaving the parking area or in bridge monitoring systems. The major problems in video monitoring systems are changing light intensities especially at late evenings and at night, weather changes like foggy atmospheres, rain, smoke etc[2]. Motion based vehicle detection can be done in different techniques such as, optical flow estimation method, Gaussian mixture model method, frame difference method and background subtraction method. After detecting only the vehicles it can also be used for classification for types of vehicles. The background subtraction is most popular because of its simplicity in implementation for vehicle detection. Here background is estimated by taking the initial two or three frames of a video and then the next frames are subtracted with this estimated background to get the moving objects in a video. The challenging part of the method is the estimation of the background because shadow, camera vibrations, change of illumination may occur and noise can get introduced. After detecting the moving vehicles it is counted by using the detection line drawn in video. The problems that can occur in counting is occlusion of two or more vehicles. Counting error can be reduced by taking care of camera angle or by taking the width of the moving objects.

In this paper simple background subtraction method is taken to detect the moving vehicles. After detecting the moving objects only vehicles are considered and it is classified and counted for traffic monitoring.

An important step in Vehicle detection is background estimation, region and feature based tracking algorithm with features to track correct objects continuously. After tracking objects their behavior and properties are recognized for analyzing traffic parameters [2].

The number of vertices per individual vehicle from the camera configuration is deduced first. Contour description model is used to describe direction of the contour segments with respect to its vanishing points, from which individual contour description and vehicle count are determined. Finally, a resolvability index to each occluded vehicle is assigned based on a resolvability model, from which each occluded vehicle model is resolved and then the vehicle dimension is measured [4].

Moving vehicles can be detected by image sequences automatically by moving object segmentation method. CC cameras are mounted at some distance from roadways; occlusion is common in traffic surveillance systems. The segmentation and recognition method uses the length, width of objects to classify vehicles as vans, utility vehicles, sedans, mini trucks, or large vehicles. Detected moving objects is recognized and counted with their varying features with the recognition and tracking methods [6].

The paper is organized as the brief review about the methods i.e. System Overview in Section 2, Experimental Results in Section 3, Conclusion in Section 4.

II. SYSTEM OVERVIEW

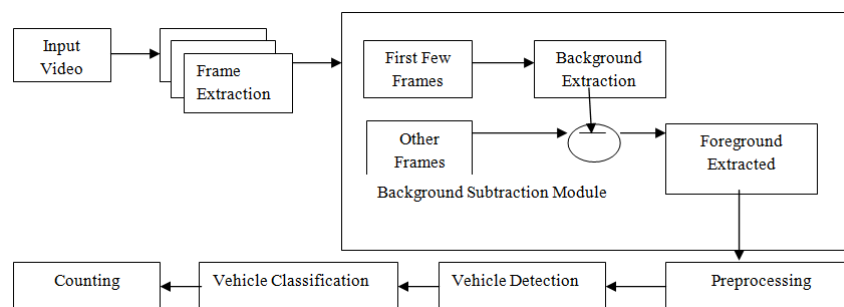


Figure 1: Block Diagram of Vehicle Detection and Counting

Fig 1 shows the block diagram for Vehicle detection and counting. From the input sequence of images, first the segmentation of moving objects from background has to be done. Image subtraction from the input sequence and background is done, which gives the changes in two frames. This method can be used only for moving objects in the input sequence, not for the objects which are idle for some time in the video.

In this work, the background subtraction method is used to segment the moving object in the scene. Background is estimated based on first few input video frames. Thresholding is used to segment the moving object from difference between the background estimated image to the current image. Morphological operations are done after the segmentation to reduce noise this is called preprocessing. After detecting the moving vehicles the bounding boxes are drawn around the vehicle. These detected vehicles are classified into car, bike or heavy vehicle. The number of vehicles is counted.

2.1 Background Estimation

The video is taken as input by reading the video from the video file present. Frame are extracted from the video, by using these frames the first few frames is taken and the average of those frames are registered as a background.

2.2 Background Subtraction

From the registered background, the other frames of the video are subtracted which gives the moving object. Some Preprocessing steps are done to extract only the moving vehicle. After background subtraction erosion, dilation and canny edge detection is applied to view the objects clearly. The mask of the moving object is taken; this can be used for classification also.

2.3 Preprocessing

Erosion and Dilation are done to view the object clearly. By erosion and dilation the boundary region of vehicles can be clearly seen. Then mask of the image can be taken for vehicle detection and classification based on the shape features.

The Dilation process is performed by laying the structuring element B on the image A and sliding it across the image in a manner similar to convolution. Dilation adds pixels to the boundaries of objects in an image by finding the local maxima and creates the output matrix from these maximum values as shown in equation (1):

$${}_1 A \oplus B = \{Z \mid (\hat{B})_Z \cap A \neq \varnothing\}$$

The erosion process is similar to dilation, but here pixels are tuned to white, not black. Erosion removes pixels on object boundaries in an image by finding the local minima and creates the output matrix from these minimum values as shown in equation (2).

$${}_2 A \ominus B = \{Z \mid (B)_Z \subseteq A\}$$

Mask: A mask is a black and white image of the same dimensions as the original image (or the region of interest you are working on). Each of the pixels in the mask can have therefore a value of 0 (black) or 1 (white). When executing operations on the image the mask is used to restrict the result to the pixels that are 1 (selected, active and white) in the mask. In this way the operation restricts to some parts of the image.

2.4 Vehicle Detection

After Preprocessing vehicle is detected. For the detected vehicles bounding boxes are drawn around the vehicle. The centroid is of the vehicle is detected and it is represented by circle on the vehicle.

2.5 Classification

Vehicle Classification is done by using the height and width ratio i.e aspect ratio, area of the vehicle. The area, height and width differs in bike, car and heavy vehicles so the classification is done based on this. Fig 2 shows the block diagram for vehicle classification.

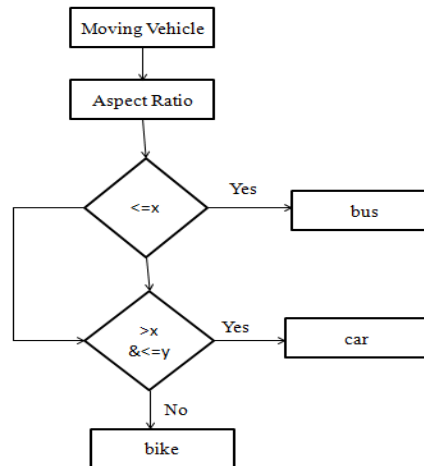


Figure 2: Vehicle Classification module

2.6 Counting

First the line is drawn as region of interest. After detecting the moving vehicle its position and centroid is detected. Whenever this centroid crosses the region of interest that is the line drawn the counter is incremented means the vehicle count is noted.

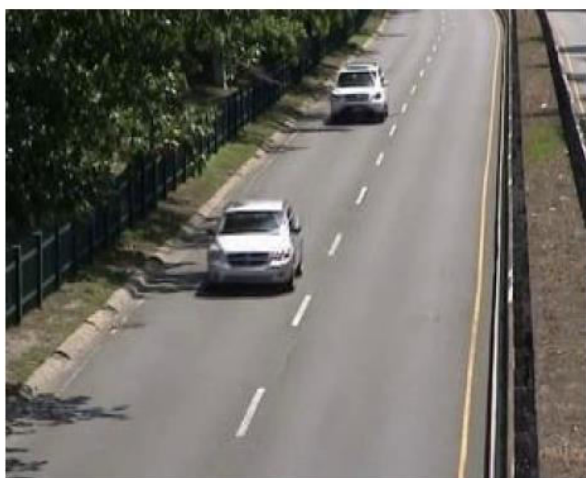
After all these steps the features of the vehicle can be extracted and classified into categories of vehicles such as car, bus, motorbike, non vehicles etc.,

Feature extraction can be done by Histogram Oriented Gradients (HoG), Principal Component Analysis (PCA). Classification can be done by using the Support Vector Machines (SVM), Latent Support Vector Machines, Neural Networks. Vehicle detection, classification and counting the vehicles with respect to their classes can be used in many areas for surveillance.

III. EXPERIMENTAL RESULTS

The experiments are conducted in Microsoft Visual Studio 2010 C++ with openCV libraries.

Fig 3.shows snapshot of a video which is taken as input and is converted into grayscale for further processing.



3a



3b

Figure3: a) Input video b) Grayscale Conversion of input

Fig 4 shows the background extracted by taking the first few frames of the video



Figure4: Background Extracted from the Video

Fig 5 shows the foreground after the frames from the video are subtracted with the background.



Figure5: Result of Background Subtraction

Fig 6 shows the morphological operations applied for better visibility of vehicle. Erosion and Dilation is applied.



a)

b)

Figure6: a) Erosion and b) Dilation Applied on Subtracted Image

Segmentation is done to get only the moving vehicle and avoiding all the static parts in video is shown in Fig 7.



Figure7: Results of Segmentation

Fig 8 shows the results of vehicle detection. The detected vehicle is represented by a bounding box.



Figure8: Results of Vehicle Detection

Fig 9a shows the detection line drawn to count the vehicles, when a vehicle crosses the line the counter is incremented that is shown in fig 9b.

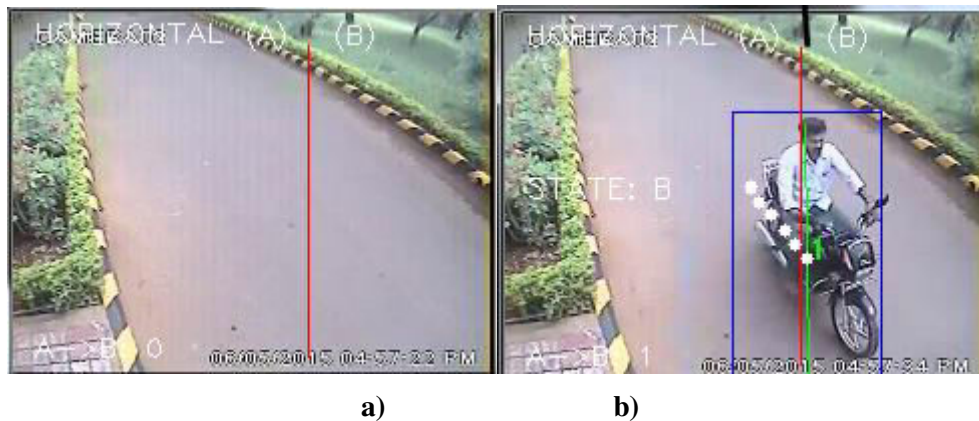


Figure9: a) Result of Drawn Detection line and b) Counting the Vehicle After it Crosses the Detection Line

Fig 10 shows the result of classification according to its aspect ratio and area.



Figure10: Results of Classification

IV. CONCLUSION

Vehicle Detection and Counting is necessary to establish an enriched information platform and improve the quality of intelligent transportation systems. In the background subtraction, moving vehicle extraction and detection, the improved background subtraction method is implemented to remove the negative impacts from camera vibration, shadow and reflection, sudden illumination changes and more gradual changes. A solution for Vehicle Detection, Classification and Counting which can be used in traffic monitoring, parking area allocation is proposed. A technique that can distinguish whether the object is vehicles or other. The experiment is carried out in Microsoft Visual Studio 2010 C++ with openCV libraries. The implemented method is easy to implement at very low expenses. Experiments give the good accuracy.

Future work is to detect 3D moving object to improve classification Performance.

REFERENCES

- [1] Huei-Yung Lin and Juang-Yu Wei, "A Street Scene Surveillance System for Moving Object Detection, Tracking and Classification", Proceedings of the IEEE Intelligent Vehicles Symposium Istanbul, Turkey, June 13-15, 2007.
- [2] Chin-Teng Lin, Fellow, Yu-Chen Huang, Ting-Wei Mei, Her-Chang Pu, and Chao-Ting Hong, "Multi-objects Tracking System Using Adaptive Background Reconstruction Technique and Its Application to Traffic Parameters Extraction", 2006 IEEE International Conference on Systems, Man, and Cybernetics October 8-11, 2006, Taipei, Taiwan
- [3] Guohui Zhang, Ryan P. Avery, Yin Hai Wang, "A Video-based Vehicle Detection and Classification System for Real-time Traffic Data Collection Using Uncalibrated Video Cameras" Department of Civil and Environmental Engineering, University of Washington Seattle, WA 98195-2700, 2006.
- [4] Clement Chun Cheong Pang, Member, William Wai Leung Lam, and Nelson Hon Ching Yung, "A Method for Vehicle Count in the Presence of Multiple-Vehicle Occlusions in Traffic Images", IEEE TRANSACTIONS ON INTELLIGENT TRANSPORTATION SYSTEMS, VOL. 8, NO. 3, SEPTEMBER 2007 441.
- [5] H'elio Palaio, Cristina Maduro, Katherine Batista and Jorge Batista, "Ground plane velocity estimation embedding rectification on a particle filter multi-target tracking", 2009 IEEE International Conference on Robotics and Automation Kobe International Conference Center Kobe, Japan, May 12-17, 2009

- [6] Chung-Cheng Chiu, Min-Yu Ku and Chun-Yi Wang,” Automatic Traffic Surveillance System for Vision-Based Vehicle Recognition and Tracking”, JOURNAL OF INFORMATION SCIENCE AND ENGINEERING 26, 611-629 (2010).
- [7] Luis Unzueta, Marcos Nieto, Andoni Cortés, Javier Barandiaran, Oihana Otaegui, and Pedro Sánchez” Adaptive Multicue Background Subtraction for Robust Vehicle Counting and Classification” IEEE TRANSACTIONS ON INTELLIGENT TRANSPORTATION SYSTEMS, VOL. 13, NO. 2, JUNE 2012 527
- [8] Zezhi Chen, Tim Ellis, Sergio A Velastin,” Vehicle Detection, Tracking and Classification in Urban Traffic” 2012 15th International IEEE Conference on Intelligent Transportation Systems Anchorage, Alaska, USA, September 16-19, 2012
- [9] Niluthpol Chowdhury Mithun, Nafi Ur Rashid, and S. M. Mahbubur Rahman,” Detection and Classification of Vehicles From Video Using Multiple Time-Spatial Images”, IEEE TRANSACTIONS ON INTELLIGENT TRANSPORTATION SYSTEMS, VOL. 13, NO. 3, SEPTEMBER 2012 1215.
- [10] Ganesh Raghtate 1, Abhilasha K Tiwari1,” Moving Object Counting in Video Signals” International Journal of Engineering Research and General Science Volume 2, Issue 3, April-May 2014 ISSN 2091-273.

RURAL WOMEN'S EMPOWERMENT THROUGH ICT FOR IMPROVING NUTRITION KNOWLEDGE AND PRACTICES

Satyapriya¹, Premlata Singh², V.Sangeetha³, Sujit Sarkar⁴ and G.S.Mahra⁵

¹Senior Scientist, ²Head and Professor, ^{3,4,5}Scientist, Division of Agricultural Extension, ICAR-IARI,
New Delhi (India)

ABSTRACT

There has been a lot of interest during the last two decades in employing Information and Communication Technologies [ICTs] for achieving sustainable agriculture and rural development. While many of these initiatives have benefited rural women by way of access to new information and new employment opportunities, women still face a number of constraints in accessing ICTs especially in the agriculture nutritional aspect. This paper explores the role of ICTs in empowering Indian rural women, through a review of ICT initiatives in India in the field of agriculture nutritional awareness. The paper concludes that, while most of the ICT initiatives are disseminating new information and knowledge useful for rural women, many are not able to make use of it, due to lack of access to complementary sources of support and services. There is immense potential for ICTs to create new employment opportunities for rural women and to contribute significant gains in efficiency and effectiveness in rural women enterprises. While ICTs can play an important role in empowering rural women, women's access and use of ICTs and empowerment clearly depends on the vision and operational agenda of the organization applying the ICTs. ICTs have become a strong ally in strengthening individuals' healthy lifestyle, taking into account nutrition intake and physical activity levels. Nutrition applications provide the means for automatic dietary intake and energy expenditure measurements as well as personalized counselling and educational services. Therefore, strengthening the ICT initiatives can go a long way in empowering rural women. Besides generating locally relevant content and enhancing the capacities of rural women in accessing ICTs, efforts are also needed to bridge the different types of digital divide [rural-urban; men-women].

Keywords: Agriculture Nutrition, ICT, Nutrition Education and Rural Empowerment

I. INTRODUCTION

Agriculture is considered a prime driver for nutrition sensitive programming because a large share of the malnourished resides in rural areas and agriculture is the source of food and other ecological services for both rural and urban people [1]. Consensus has been reached to explore all possible ways through which agriculture may achieve nutrition sensitivity. Agriculture is considered as a direct and indirect source of food at household level, as a driver of food prices; as an entry-point for enhancing women's control over resources, knowledge and status. Reviews conducted over the past several years indicate that the overall evidence base for these pathways is weak, especially in regards to anthropometric data. The studies that do exist are usually poorly powered due to sample size and time frame [2]. Largely overlooked by past research is the question of how to incentivize farmers and other professionals working in agriculture to include nutrition in their objectives [3]. Also largely

overlooked is the related question of what is logistically feasible in terms of evaluation. As most conventionally designed agricultural projects do not include nutrition indicators in their design, there are little evaluative data available on the subject. This is one of the reasons for the weak evidence base and, when considered within the context of the incentives issue, poses a challenge to proponents of nutrition sensitive agriculture. Another reason is that farm women are having various constraints in attaining agriculture nutrition education or knowledge. Following table explains the reach of farm women in attaining any agricultural technology.

Table 1: Rural Farm Women Accessing Modern Agricultural /Nutritional Technology

S. No	Source	% of hrs
1.	Participation in Training	0.9
2.	Krishi Vigyan Kendra [KVK]	0.7
3.	Extension worker	5.7
4.	Television	9.3
5.	Radio	13.0
6.	Newspaper	7.0
7.	Village fair	2.0
8.	Government demonstration	2.0
9.	Input dealer	13.1
10.	Other progressive farmers	16.7
11.	Farmers' study tour	0.2
12.	Para-technician / private agency / NGO	0.6
13.	Primary cooperative society	3.6
14.	Output buyers / food processor	2.3
15.	Credit agency	1.8
16.	Others	1.7
17.	Any Source [all of the Above]	40.4

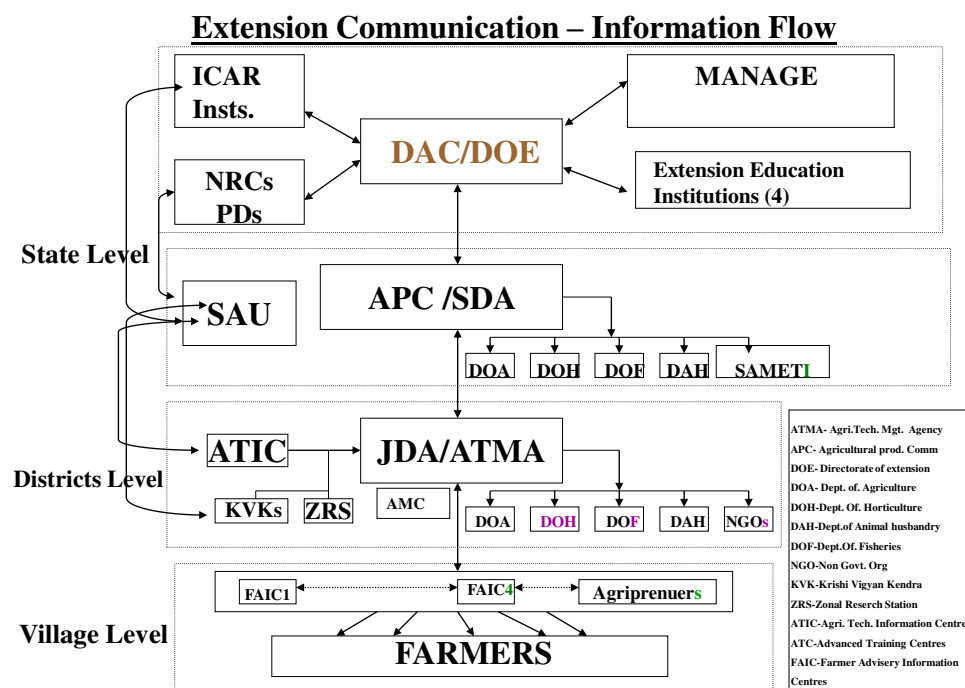
1.1 Empowerment of Rural Women

Empowering rural women is considered absolutely fundamental to increasing nutrition sensitivity in agriculture as women make up a large percentage of the agricultural labor force in developing countries. Beside this the resources and income flows that women control have been shown to have disproportionately positive impacts on nutrition security, [4]. The key areas through which women can exercise their autonomy in agriculture are: agricultural production; resources and assets; income; leadership and time allocation [5]. Although women's empowerment in each of these domains poses challenges, time allocation is of particular concern because women's increased participation in paid and unpaid agricultural labor reduces time spent on activities that affect household nutritional status, namely caring for children, food preparation, water and fuel collection, shopping, housekeeping, and family health care. As such, it is critical to take a "do no harm" approach to guard against the unintentional negative consequences of agriculture based activities aiming to promote gender equality. In addition to the issue of time allocation, other risks include gender-based violence as well as the ill-health effects that can come from working in unsafe agricultural environments. In order to avoid these unintended

consequences, identification and tracking of potential “gender harms”, together with development of a feasible mitigation plan, are essential to agriculture programmes aspiring to nutrition sensitivity.

Integrating nutrition education into agricultural and food system interventions which aspire to nutrition sensitivity is essential to achieving the social and behavioral change necessary for improved nutrition practices. This is because improved food security and purchasing power, while certainly associated with improved nutrition, may not be enough, in and of themselves, to improve nutrition outcomes [6]. Simply put, improved access and availability do not automatically translate into improved dietary intake. This fact underlies the entire premise of nutrition sensitive programming in agriculture.

In India, Government has taken number of initiatives for nutritional security among rural mass. But, agriculture nutritional programme or information are going through a long chain and takes a lot of time and energies. It is not possible to knock every door of rural farm women to educate them about nutritional sensitivity with existing model.



Hence, contemporary nutrition-related issues in conjunction with innovations in information and communication technologies [ICTs] are the core-elements of the present state of- the-art article. In an attempt to address to the societal needs for continuous health and nutrition preserverence and care, ICTs provide the means to the realization of effective state policies and scientific interventions. Target audience of such applications is individuals at home or at work as well as professional caregivers. In both cases, the goal of the nutrition interventions implemented should be lifestyle- oriented. In order to fulfill these goals, applications should enhance end-users’ self-monitoring and self-management skills. ICTs are an in adversely strong determinant factor as to the massive, immediate and low-cost deployment of nutrition-related interventions. Nutrition applications go far beyond the boundaries of mere consumption of low-calorie foods and one-way dietary interventions. They have to do with individuals’ physical and psychological health as a unity. Therefore, manual, visual or audio dietary intake entry combined with activity level recordings or total energy expenditure measurements, should both be accompanied by counseling for raising self-awareness and self-efficacy levels. In

essence, individuals are trained to change their behaviour by realizing their nutritional and lifestyle, less beneficiary habits. During the whole process, support and guidance are predictive factors of long-term engagement in a program. That is the reason why nutrition applications should adapt to individuals' personal profile and character for goal setting as well as for intervention evaluation purposes. Tailored feedback towards individuals has been found to raise their accountability and offer them encouragement. Thus, the more personalized the feedback the more effective the intervention. Effective applications should therefore be interactive in order to maintain individuals' interest as well as flexible and reusable in order to apply to as many individuals as possible at the minimum cost. Individuals' motivation is also enhanced through accessible, convenient and reliable applications, especially for multi-variable settings, such as life-long diseases and/or socially impaired target groups, who come up against a variety of everyday adversities. Professional careers are also in need of such applications as they seek to satisfy their constant need for efficient and high-quality counseling services. In general, nutrition applications provide quality and standardization of health intervention studies in an attempt to improve all people's nutritional and lifestyle behaviors.

II. REVIEW OF ICT APPLICATIONS: The different ICT based applications in the field of nutrition security are presented below-

2.1 Mobile Based Nutritional Awareness

Today, mobile is the strongest and fastest medium to reach the unreached for agriculture nutritional awareness. Though, use of mobile for nutritional awareness for rural youth in India still needs attention. But, for advisory services in other allied activities of agriculture is gaining popularity. In developed countries a lot of initiatives were taken in this regard. Hebden et al, describe the process of developing four smartphone applications to raise young adults' motivation in the improvement of their nutrition and physical activity behaviours [7]. The purpose of the applications was to enhance subjects' self-reflection on their physical activity and consumption of take-out foods [fast food], fruit, vegetables and sugar-sweetened drinks. The realisations of such intriguing, cost-effective, long-term health interventions, focusing on subject's self-assessment and awareness, necessitate, therefore, continuous encouragement and support in the form of personalised feedback. Kerr et al., reported that a 6-month nutrition intervention project aiming at young adults' improvement of eating behaviors, makes use of a mobile application called "CHAT" that keeps a record of the food images consumed as well as invites the intervention group to perform dietary changes through tailored feedback on their food intake via a text message [8]. In this case, nutritional messages referred to consumption of fruit, vegetable and junk food are related to age, gender and behavioral characteristics. Not only are the content, frequency and length of text message important, but also the adequate time of receiving it in order for the participants to build their self-efficacy on healthy eating habits. Vandelanotte et al. [9] performed a pilot-study concerning middle-aged, Australian men views on mobile phone delivered physical activity and nutrition interventions. Middle-aged men prefer tailor-made, self-monitoring and intervention delivery applications performed especially in smartphones, with an emphasis on maximum simplicity, speed and convenience in their operation. Medhi et al., [10] present observations and findings from a three-month field study in rural India, during which an easy-to use application, deployed in low-cost mobile phones, substituted paper-based data for a more accurate and accessible, digital database concerning the combat against children's malnutrition. Data entry and management was upgraded, whereas infrastructure deficiencies should be diminished by staff training and easy-to access technical support.

2.2 Web Based Nutrition Expert System

It is very effective tool and can be implemented at community level with little hands of training. In this area, search is centered in the development of multi-level systems, designed to offer multi-purposed services for covering a variety of needs on behalf of their users. Much advanced form of this application are using at rural and urban areas in developed countries. Chena *et al.*, [11] launches a web-based nutrition diagnosis expert system for dietetic professionals in Taiwan. This expert system assists in the nutrition-related decision making. Agri -Nutrition expert system offers a holistic approach in nutrition diagnosis and management, as it comprises both identification of the problem and the means to deal with it in a standardized, profound and efficient way . Lewis et al. argue that information technology may influence consumers' food choices by increasing their personal interest in looking after their own health status [12]. Especially, hand-held devices or phones could record daily nutrient information during food intake and furthermore, a more personalized profile of the consumers' nutritional needs would be possible. Also, devices such as the 'bodybugg' that measures the total energy expenditure of a whole day and sends it to an online database could provide the interested party with the necessary feedback in order to achieve body weight goals. Koch et al. bring to light an expanding, cross-disciplinary research subject concerning the delivery of care to older people, such as their nutrition, physical activity and medication with the assistance of information technology, sensor technology, and information systems [13]. It seems that elderly population's perspectives towards their care differentiate according to the stage of their aging process as well as to their gender. Lopez et al., motion sensors inside a mobile phone convert accelerometry counts into energy expenditure by taking into account heart rate, body and environment temperature under free-living conditions [14]. Bickmore et al. launch an ontology of health behavior change, deployed for diet promotion [15]. The notable efficacy of this automated, media-based intervention is attributed both to its capacity to emulate the behaviour of an expert counsellor and to its reusability and interoperability. In this way, patients' health behavior change applications can become a strong health counseling tool, taking into account the reduction of their dissemination cost. Takahashi et al. present an Automatic Nutrient Calculation System on the web, which identifies and calculates the amount of the ingredients in grams included in almost 1 million registered recipes as well as the total amount of nutrients in each one of the ingredients [16]. Amft et al. argue that on-body sensors can make rough estimations on ratio of fluid and solid foods consumed and also they can capture food category and timing information [17]. Thus, behavioral-based, nutrition interventions can become more solid and precise. The three sensing domains are arm and trunk movements, chewing of foods and swallowing activity. Evidently, recognition of dietary activity events was realized by means of quantitative detection and classification, accounting for automatic dietary monitoring. Ayres et al. made a record on the necessary nutrition informatics competencies in dietetics. Informatics includes the efficiency to collect, store, retrieve and study data [18]. Nutrition informatics is the intersection of information, nutrition, and technology, a future-holding, cross-disciplinary innovation in dietetics and health care in general. In Delphi study presented, registered dietitians are convinced of the fact that they should be able to select, implement and maintain sufficiently, information management systems across all levels of their practice.

2.3 TELE Based - Agri Nutrition Education

Applications belonging in telenutrition research field are easy-to-use and cost-effective, as they enhance the adaption of long-lasting, self-monitoring health behavior change. Herberg et al. investigate the relationship between nutrition and health outcomes in a 10-year follow-up, web based study called "The Nutrinet-Sante

Study”, located in France [19]. At the starting point of the study, volunteers record three 24h dietary intake, socio-demographic and lifestyle questionnaires, health, anthropometric questionnaires and physical activity questionnaires. Every year, the participants must once again fill in the abovementioned questionnaires as well as the three 24h dietary records. Moreover, every month they will receive informative e-mails, reminding them of the necessity to update their personal profiles on their food behaviour, nutritional and health by filling out a new questionnaire via the website. Neuenschwander et al. made a comparative study between a web-based and an in-person nutrition education program for low-income adults. The technical part of the interventions, such as their content and duration was similar. Traditional in-person nutrition education and web based nutrition education, both showed significant nutrition- related behaviour outcomes [20]. Moreover, the nutrition related changes were equivalent in both intervention groups. Web-based participants also reported willingness to use the website again, taking into account its efficacious design, decreased cost of accessibility and easy implementation. Vandelanotte et al. made a pilot-study aimed to examine middle-aged, Australian men’s opinions and perceptions regarding the use of internet in the improvement of their physical activity and nutrition behaviors. It is noteworthy that the aforementioned target group show low commitment levels to engagement in health intervention programs. Indeed, middle-aged men support the use of websites as a means to self-monitor their physical activity and nutrition behaviours on the condition that delivered interventions are accessible, understandable, appealing, reliable and concise [21]. Gibney et al. argue that the use of web-based, personalized nutrition applications for the collection of food data in an intervention study should be, first of all, plausible and user-friendly, even though precise and exact data entry from the participants is less possible. Furthermore, personalized feedback towards the participants should be easy-to-use, based on simple visual tools, instead of any numeric data. Food choice advice should be focused on meal intake and ranges of nutrient intake, presented on the computer screen by making a classification, depending on the participant’s average nutritional needs [22]. Hong et al. created a kid-friendly, web-based nutrition education searching system, combining both video scripts of the cooking process of healthy recipes and easily learned nutrition information with plenty of searching methods. Children can seek for a menu of their preference by using a key word expression such as food materials, age group, menu type, menu style and nutrients or the upper and lower bound of the calories and the nutrients they opt for. Hong et al. created a web expert system for nutrition management and counselling, which takes into consideration gender, age and diseases so as to compose general and therapeutic meals. The system compares e-databases, originating from user’s information and experts’ recommendations in the sense that the latest assess on-line the nutrients and calories included in a meal, chosen by the user of the system [23]. Vereecken et al. made a comparative study on the feasibility of young children’s nutrition assessment, based on their dietary habits and their parents’ sociodemographic variables, by implementing either an on-line assessment tool or a paper and pencil questionnaire. No significant differences were found in relation to nutrient and food group recordings, except from water. Parents that preferred to fill in the pencil food diary were younger and had a lower education level. From the parents that completed the on-line questionnaire, the majority indicated that it was user-friendly, attractive and clear [24].

III. INDIAN CONTEXT

Presently in India most of the agriculture nutrition education or awareness programmes are going through personal contacts, campaign, print media [newspaper, wall paintings, leaflets etc.,] or e- media like television or

radio. For speedy and cost effective transfer of nutritional technologies or to create agri - nutritional awareness for empowerment of rural women's, other effective tools can be Kissan Call Centre, Community Radio Stations, Farmers Kiosk at village level, expert system in online and offline mode and different multimedia models. There is an urgent need to develop ICT based tools in line with our traditional and healthy nutrition practices in the Indian context.

TABLE 2: Area of Application of ICT in Nutritional Empowerment

S.No.	ICT Tools	Application
1.	Mobile	<ul style="list-style-type: none"> • Audio-Video messages through mobile phones, mobile apps, alert calls regarding nutritional uptake of rural mass and regular health checkups • Package of practices of nutrient rich varieties • Monitoring and feedback mechanism through mobile based applications
2.	Web	<ul style="list-style-type: none"> • Dissemination of recommended dietary requirement [carbohydrate, protein, fat, vitamin , minerals and dietary fibre) to rural mass • Nutritional Campaigns organization and mass awareness in villages
3.	Expert System	<ul style="list-style-type: none"> • To analyse the dietary intake and calorie requirement • To analyse the required quantity carbohydrate, protein, fat, vitamin, minerals and dietary fibre • Content Development regarding best nutrition practices
4.	Nutritional Portal	<ul style="list-style-type: none"> • All sources of different nutrients according to age group • Package of practices of nutrient rich varieties • Nutrition related diseases and cure
5.	e-Video Library	<ul style="list-style-type: none"> • Best Cooking practices of vegetables and nutria rich foods • Various nutrient rich diet combinations according to age group • Development of Multimedia CD's

IV. CONCLUSION

Most of the ICTs are disseminating new information and knowledge on agriculture, health and nutrition among rural women. However, due to the continuing digital divide between urban and rural areas and also between men and women, many rural women are yet to fully benefit from the potential of ICTs. Research data on nutrition & ICTs show the importance of behaviour-based applications in individuals' health preservice. Dietary intake and physical activity in everyday life are both constituents of a healthy lifestyle. Self regulatory skills are vital for life-long behavioural changes. Nutrition applications should also be genuinely intriguing as they need to provoke individuals' long-term engagement in an intervention program. For that purpose, personalized communication as well as tailored feedback according to individuals' personal profile, are predominant for treatment alterations and psychological support. Moreover, flexible, multiple purpose and cost-effective nutrition applications offer the opportunity of serving the needs of a large number of the population at a low cost, thus enhancing preventive medicine and reducing the inherent difficulties of the deprived part of the society. Finally, such applications should be accurate and trustworthy in order to gain interested party's

acknowledgement and acceptance, ranging from healthcare professionals to individuals, concerned about their health status.

While new information and knowledge is necessary, it is not sufficient to bring about women empowerment. To make use of the information, women would need access to other sources of support and services. Women who are part of other development initiatives or groups and those who have access to other sources of service and support were able to better use the information and knowledge disseminated through ICTs. The potential of ICT tools varied widely in reaching rural women. There is no ideal ICT tool that fits all situations. Need to develop a basket of ICTs effective tools to empower rural farm women's through nutritional awareness under various agriculture nutritional projects

REFERENCES

- [1] Herforth, A., Jones, A., Pinstrup-Andersen, P. 2012. *Prioritizing Nutrition in Agriculture and Rural Development: Guiding Principles for Operational Investments*. Washington DC: World Bank.
- [2] Ruel, M.T., Alderman, H. and the Maternal and Child Nutrition Study Group. 2013. *Nutrition-sensitive interventions and programmes: how can they help to accelerate progress in improving maternal and child nutrition?* The Lancet - 6 June 2013.
- [3] Meeker, J., Haddad, L. 2013. *A State of the Art Review of Agriculture-Nutrition Linkages: An AgriDiet Position Paper*. Brighton: Institute of Development Studies.
- [4] World Bank. 2007. *From Agriculture to Nutrition: Pathways, Synergies and Outcomes*. Washington DC: World Bank.
- [5] Alkire, S., Meinzen-Dick, R., Peterman, A., Quisumbing, A., Seymour, G., Vaz, A. 2012. *The Women's Empowerment in Agriculture Index*. IFPRI Discussion Paper 01240. Washington DC: IFPRI.
- [6] IYCN. 2011. *Nutrition and Food Security Impacts of Agriculture Projects*. Washington, DC: United States Agency for International Development.
- [7] Hebden L., Amelia Cook A., Van der Ploeg H. P. & Margaret Allman-Farinelli M. : "Development of Smartphone Applications for Nutrition and Physical Activity Behavior Change", *JMIR Res Protoc* 2012, vol. 1, issue 2, e9, [2012].
- [8] Kerr D. A., Pollard C. M., Howat P., Delp E. J., Pickering M., Kerr K. R., Dhaliwal S. S., Pratt L. S., Wright J. & Boushey C. J. : "Connecting Health and Technology [CHAT]: protocol of a randomized controlled trial to improve nutrition behaviours using mobile devices and tailored text messaging in young adults", *BMC Public Health*, vol. 12, issue 477, pp. 1-10, [2012].
- [9] Vandelanotte C. , Caperchione C. M., Ellison M., George E. S., Maeder A., Kolt G. S., Duncan M. J. , Karunanithi M. , Noakes M. , Hooker C., Viljoen P. & Mummery W. K. : "What Kinds of Website and Mobile Phone-Delivered Physical Activity and Nutrition Interventions Do Middle-Aged Men Want?", *Journal of Health Communication*, pp. 1-14, [2013].

- [10] Medhi I, Jain M., Tewari A., Bhavsar M., Matheke-Fischer M. & Cutrell E. : “Combating Rural Child Malnutrition through Inexpensive Mobile Phones”, NordiCHI’12, October 14-17, 2012 Copenhagen, Denmark.
- [11] Chena Y., Hsua C.-Y., Liua, L., Yangb S. : “Constructing a nutrition diagnosis expert system”, Expert Systems with Applications, vol. 39, issue 2, pp. 2132–2156, [2012].
- [12] Lewis K. D. & Burton-Freeman B. M. : “The Role of Innovation and Technology in Meeting Individual Nutritional Needs”, The Journal of Nutrition, vol. 140, pp. 426-436, [2010].
- [13] Koch S. & Hägglund M.: “Review: Health informatics and the delivery of care to older people”, Maturitas, vol. 63, issue 3, pp. 195–199, [2009].
- [14] Lopez L. J. R., Goroso D. G. and Battistella L. M. : “Sensor Network for Assessment of Energy Expenditure design based on Android CLAIB 2011”, IFMBE Proceedings, vol. 33, pp.678–681, 201, [2011].
- [15] Bickmore T. W., Schulmana D. & Sidnerb C. L. : “A reusable framework for health counseling dialogue systems based on a behavioral medicine ontology”, Journal of Biomedical Informatics, vol. 44, issue 2, pp. 183–197, [2011].
- [16] Takahashi J., Ueda T., Nishikawa C., Ito T. & Nagai A.: “Implementation of Automatic Nutrient Calculation System for Cooking Recipes Based on Text Analysis”, PRICAI 2012, LNAI 7458, 789–794, [2012].
- [17] Amft O. & Tröster G. : “Recognition of dietary activity events using on-body sensors” Artificial Intelligence in Medicine, vol. 42, issue 2, pp. 121–136, [2008].
- [18] Ayres E. J., Greer-Carney J. L., McShane, F. P. E., Miller, A. & Turner P. : “Nutrition Informatics Competencies across All Levels of Practice: A National Delphi Study”, Journal of the Academy of Nutrition and Dietetics, vol. 112, issue 12, pp. 2042–2053, [2012].
- [19] Hercberg S., Castetbon K. Czernichow S., Malon A. Mejean C., Kesse E., Touvier M. & Galan P. : “The Nutrinet-Sante Study: a web-based prospective study on the relationship between nutrition and health and determinants of dietary patterns and nutritional status”, BMC Public Health, vol. 10, issue 242, pp. 1-6, [2010].
- [20] Neuenschwander, Author Vitae L. M., Abbott, A. & Author Vitae Mobley, A. R. : “Comparison of a Web-Based vs In-Person Nutrition Education Program for Low-Income Adults”, Journal of the Academy of Nutrition and Dietetics, vol. 113, issue 1, pp. 120- 126, [2013].
- [21] Vandelanotte C. , Caperchione C. M., Ellison M., George E. S., Maeder A., Kolt G. S., Duncan M. J. , Karunanithi M. , Noakes M. , Hooker C., Viljoen P. & Mummery W. K. : “What Kinds of Website and Mobile Phone–Delivered Physical Activity and Nutrition Interventions Do Middle-Aged Men Want?”, Journal of Health Communication, pp. 1–14, [2013].
- [22] Gibney M. J and Walsh M. C. : “The future direction of personalized nutrition: my diet, my phenotype, my genes”, Proceedings of the Nutrition Society, vol. 72, pp. 219–225, [2013].

- [23] Hong S.-M., Cho J.-Y., Lee J.-H., Kim G. & Kim M.-C. : “NutriSonic web expert system for meal management and nutrition counselling with nutrient time-series analysis, e-food exchange and easy data transition”, Nutrition Research and Practice, vol. 2, issue 2, pp. 121-129, [2008].
- [24] Vereecken C. A., Covents M., Haynie D. & Maes L. : “Feasibility of Young Children’s Nutrition Assessment on the Web”, J Am Diet Assoc, vol. 109, issue 11, pp. 1896-1902, [2009].

MULTIMODAL BIOMETRIC SYSTEM COMBINING MATCHING SCORE LEVEL AND FEATURE LEVEL FUSION

Vinay Kumar. M. S¹, Dr. R. Srikantaswamy²

¹PG Scholar, ²Professor, Dept of ECE, Siddaganga Institute of Technology,
Tumakuru, Karnataka, (India)

ABSTRACT

Nowadays, Multimodal biometrics has created a substantial interest in the field of identification management due to higher recognition performance. This paper combines the matching score level and feature level fusion in order to develop a multimodal biometric system for face and fingerprint biometrics. Histogram of Oriented Gradients (HOG) descriptor has been used for fingerprint recognition, Viola-Jones algorithm for face detection and Linear Discriminant analysis (LDA) along with Principal component analysis (PCA) for face recognition. The features extracted from the fingerprint and face biometrics are combined at matching score level and feature level. We have combined matching score level fusion and feature level fusion for verification and identification respectively. And the system yields good verification and recognition performance when compared to other multimodal and unimodal biometric systems.

Keywords: *Face detection & recognition, Fingerprint recognition, Multimodal biometrics, Feature level, Score level.*

I. INTRODUCTION

Biometric Technology is an automatic technique of recognizing a person based of one (Unimodal) or more (Multimodal) behavioral or physiological characteristics. An authentication system is now a part of almost every major information technology. Biometric technology has become the foundation for highly secure person verification and identification. The global-state of information security survey reveals that the security breaches are on rise. Unimodal biometric systems can be hacked easily and it suffers from the problems like noisy sensor data, non-universality, intra-class variation, lack of individuality and spoofing attacks. Multimodal biometrics [1][2] has additional information regarding various discreet modalities which in turn increases the recognition performance in terms of accuracy and also to overcome the drawbacks associated with unimodal biometrics. A combination technique is necessary which fuses information from diverse modalities so as to have a multimodal biometric system. There are four levels of fusion techniques viz., fusion at sensor level, fusion at feature level, fusion at matching score level and fusion at decision level[3][4][5]. But the fusion at sensor level is used very rarely and also not compatible in most of the applications.

Many fusion strategies has been proposed by several authors [6-9][10-12]. In this paper, a robust multimodal biometric system using face and fingerprint modalities (as each of the modalities are unique and consistent over time) which are combined at feature level fusion and matching score level fusion is proposed.

In this paper, we have used pattern based fingerprint recognition using the Histogram of Oriented Gradient (HOG) descriptors which was used in computer vision for object recognition purpose and for face we have used a robust face recognition method called Linear Discriminant Analysis (LDA). In order to ensure better recognition, we have cropped the face region from the background using the Viola-Jones face detection method. Later, features and scores are computed from each of the modalities. The individual scores are normalized and combined using min-max normalization technique and weighted sum rule respectively. If the query face and fingerprint are verified then the features extracted from those modalities are passed to feature level fusion for recognition. Features extracted are combined using feature concatenation method and these features are combined in such a way that even though the imposter gains the access in the verification stage still we can comprehensively identify the imposter in the identification stage, thus making the proposed system more robust to illegal access. These combined features are given to multi-class Support Vector Machine (SVM) for classification.

The rest of the paper is organized as follows, Chapter 2 discusses a feature extraction method for both face and fingerprint. Chapter 3 describes the matching score level fusion and feature level fusion is discussed in Chapter 4. Proposed structural flow of the methodology is explained in Chapter 5. Experimental results are given in Chapter 6 and Chapter 7 provides the conclusion.

II. PROPOSED FEATURE EXTRACTION TECHNIQUES FOR FINGERPRINT AND FACE

2.1 Fingerprint Recognition

HOG methodology is mainly based on evaluating well-normalized local histograms of image gradient orientation in a dense grid with 50% overlapping blocks. HOG features are calculated by taking orientation histograms of edge intensity in local region. The basic thought is that local object appearance and shape can often be characterized rather well by the distribution of local intensity gradients or edge directions, even without precise knowledge of the corresponding gradient or edge positions. The Structural flow for fingerprint recognition is as shown in Fig 1.

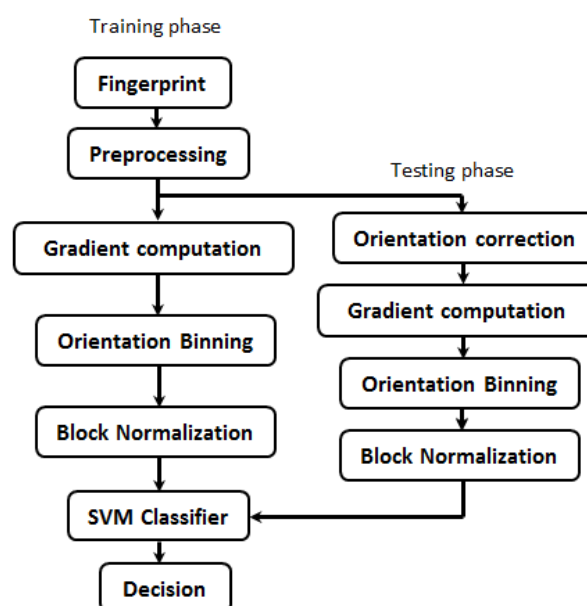


Figure 1. Flow for Fingerprint Recognition

In preprocessing stage, the fingerprints acquired are subjected to sharpening into order to enhance the ridge details as this method is mainly based on ridges and the sharpened image is converted into binary. The fingerprint image is divided into 3×3 blocks. For each block, gradients along X and Y directions are calculated (I_x and I_y) using 1-D Gaussian kernels $d_x=[-1,0,1]$, $d_y=[-1,0,1]^T$. The magnitude and gradient orientations are computed using (1) and (2):

$$I_{mag} = \sqrt{I_x^2 + I_y^2} \quad (1)$$

$$\theta = \arctan\left(\frac{I_y}{I_x}\right) \quad (2)$$

The gradient orientations are quantized into 9 bins. Each pixel within the cell casts a weighted vote for an orientation based histogram channels and the histogram channels are evenly spread over 0 to 360 degrees. The gradient magnitude calculated for each pixel gives the weighted vote. In order to take care of illumination (in this case, pressure variation), each blocks are locally normalized using L-1 norm using (3):

$$f = \frac{v}{\|v\|_1 + e} \quad (3)$$

HOG features extracted from the fingerprints are given to SVM for training. During the testing phase, an ellipse is fitted on to the query fingerprint in order to find the orientation of the fingerprint. The orientation of the fingerprint is found out by calculating the orientation of major axis for the ellipse that has been fitted earlier. If the orientation angle is within the acceptable range then no action will be taken, if it exceeds the acceptable range (shown in Fig.2) then the fingerprint image has to be rotated with same angle but in opposite direction to that of the inclination angle. After orientation correction, the region of interest is extracted and image is resized to actual dimension of the fingerprint image.

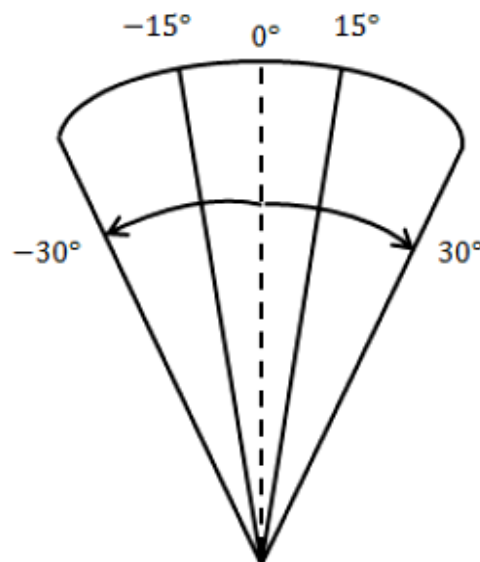


Figure 2. Maximum Acceptance Angle

Fingerprint will be corrected if the inclination of major axis is in between $\pm 15^\circ$ and $\pm 30^\circ$. A feature extracted from the corrected fingerprint is given to the SVM for classification. Brief description of HOG descriptor on fingerprint is as shown in Fig. 3.

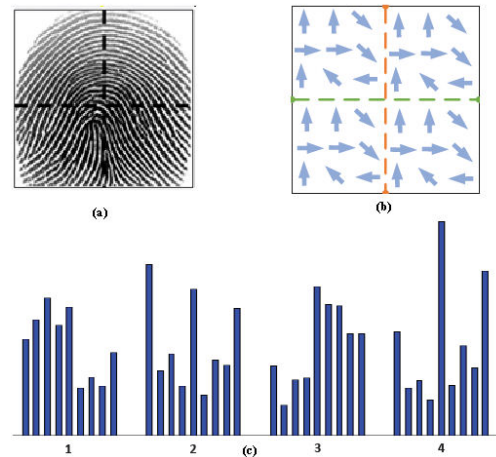


Figure 3. Brief Description of HOG Descriptor (A) Fingerprint Image Divided into 4 Blocks (B) Gradient Orientation of Each Block (C) Histogram of Oriented Gradients

2.2 Face Recognition

The facial features are extracted from the face images using Fisher's linear discriminant analysis (FLDA) technique. FLDA gives importance to those vectors in the underlying space that best describe the best discriminate among classes rather than best describing the data. It makes the projection from high dimensional image space to a low-dimensional image space and tries to maximize the ratio of between-class scatter matrix and the within-class scatter matrix as shown in Fig 4.

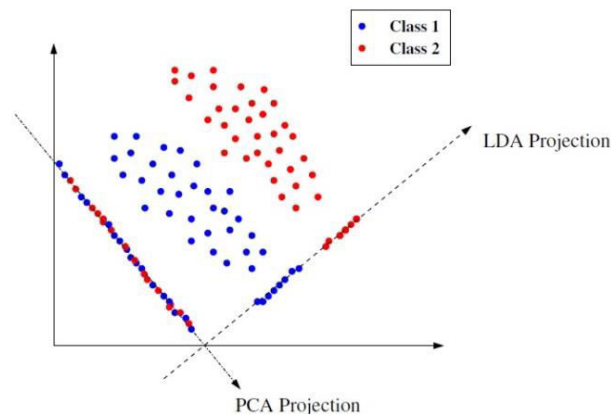


Figure 4. PCA and LDA Projection of Two Class Problem

Fisher's face method has been used for face recognition which is robust to illumination and poses variation. As a preprocessing step we have used Viola-Jones face detection algorithm[13] which detects the face and the detected face is cropped from the background region. This cropped face is used for feature extraction and it is given to Euclidean distance classifier. It calculates the Euclidean distance between the query image and the templates that is stored in the database and assigns the query image to the template which ever yields the minimum distance. The flow for face recognition is as shown in Fig 5.

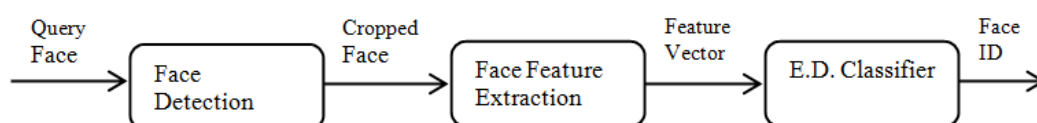


Figure 5. Flow for Face Recognition

Let us consider R face images of C individuals (classes) in the training set and each image X_i is a 2-D array of size $m \times n$ of intensity values. An image X_i is transformed into a vector of D ($D=m*n$). Defining the training set of R images by $X = (X_1, X_2, \dots, X_R) \in \mathfrak{R}^{D \times R}$. The between-class scatter matrix is defined as follows:

$$C_B = \sum_c N_c (\mu_c - \bar{X})(\mu_c - \bar{X})^T \quad (4)$$

Where, N_c is number of images in class c , μ_c , and \bar{X} are the mean images of the c class and training images, respectively. They are defined as follows:

$$\mu_c = \frac{1}{N_c} \sum_{i \in c}^R X_i \quad (5)$$

$$\bar{X} = \frac{1}{R} \sum_i^R X_i \quad (6)$$

The within-class scatter matrix is defined as follows:

$$C_W = \sum_c \sum_{i \in c}^R (X_i - \mu_c)(X_i - \mu_c)^T \quad (7)$$

The Fisher's criterion is defined as follows:

$$F(W) = \frac{|WC_B W^T|}{|WC_W W^T|} \quad (8)$$

If C_W is a non-singular matrix then this ratio is maximized when the column vectors of the projection matrix W , are eigenvectors of $C_B C_W^{-1}$. The optimal projection matrix W_{opt} is defined as follows:

$$W_{opt} = \underset{W}{\operatorname{argmax}} |C_B C_W^{-1}| \quad (9)$$

$$= [w_1, w_2, \dots, w_m]$$

Where $\{w_i \mid i = 1, 2, \dots, m\}$ is the set of normalized eigenvectors of $C_B C_W^{-1}$ corresponding to m largest eigenvalues $\{\lambda_i \mid i = 1, 2, \dots, m\}$. Each of the m eigenvectors is called Fisherface.

If C_W is a singular matrix, then the projection has to be made to a lower dimensional space so that resulting within-class scatter matrix C_W is non-singular. This is achieved by using PCA to reduce the dimension of the feature space to $R-C$ and then applying the standard FLD to reduce the dimension to $C-1$. After calculating the optimal weights, these weights are given to Euclidean distance classifier. W_{opt} is given by:

$$W_{opt} = W_{fld} W_{pca} \quad (10)$$

$$\text{Where, } W_{fld} = \underset{W}{\operatorname{argmax}} \frac{|W^T W_{pca}^T C_B W_{pca} W|}{|W^T W_{pca}^T C_S W_{pca} W|}$$

$$W_{pca} = \underset{W}{\operatorname{argmax}} |W^T C_T W|$$

III. MATCHING SCORE-LEVEL FUSION

In our methodology, matching score level fusion is used to address the problem of verification. The scores of fingerprint image is obtained using the concept of feature matching i.e., given a feature of one image, finding out the best matching feature in one or more images. Absolute difference is computed between the feature extracted from the query image and the features of the training images stored in the database which results in a single vector. Summing up all the rows in the difference vector to get a single scalar score. Continuing this process for all the training features and score for each query fingerprint are calculated using the best feature match (smallest score) and the second best feature match (2nd smallest score).

$$\text{Score} = \frac{\text{Score of best feature match}}{\text{Score of second best feature match}} \quad (11)$$

The scores for query face can be obtained easily by finding the minimum Euclidean distance between each query face and the face template which is stored in database. The minimum Euclidean distance is itself taken as distance score.

In the context of verification, there are two approaches for consolidating the scores obtained from different matchers. One approach is to formulate it as a classification problem, while the other approach is to treat it as a combination problem. In classification approach, a feature vector is constructed using matching scores output by individual matchers; this feature vector is then classified into one of two classes: "Accept" or "Reject". In combination approach, the individual matching scores are combined to generate a single scalar score which is then used to make the final decision. In order to ensure meaningful combination, all the scores must be transformed into common domain using any of the normalization techniques.

We have used a combination approach for the score level fusion. Before combining the scores, scores has to be normalized in order to transform the scores into same numerical range as the scores obtained from the fingerprint and face are similarity scores, dissimilarity scores respectively. Here we have used min-max normalization technique as this method is best suitable for the case where the bounds (minimum and maximum values) of the scores produced by the matcher are known. The normalization procedure shifts the scores between {0,1}. Let s_{ik} be a vector which contains the score of individual modality. Let s_{ik} and s_{ik}' be the un-normalized test score and normalized test score calculated using (11):

$$s_{ik}' = \frac{s_{ik} - \min(\{s_i\})}{\max(\{s_i\}) - \min(\{s_i\})} \quad (12)$$

The scores of both fingerprint and face are normalized using min-max normalization technique. And these normalized scores are combined using weighted sum fusion rule with equal weights ($\alpha = \beta = 0.5$).

$$\text{FinalScore} = \alpha * \text{normalized face score} + \beta * \text{normalized finger score} \quad (13)$$

In order to make decision, threshold has been set which well discriminates the genuine and imposter scores. If final score < threshold, that score is characterized as imposter and if final score > threshold, that score is characterized as genuine.

IV. FEATURE LEVEL FUSION

Feature level fusion addresses the problem of both verification and identification. In our method, we are using this fusion level to solve the problem of identification. The features extracted from the face and fingerprint modalities using LDA and HOG are serially concatenated in order to combine them. The features are fused in such a way that, even though the imposter succeeds in verification stage he can be easily rejected in identification stage thus, making the proposed algorithm robust and dynamic. Let Y_{face} be the face feature vector extracted by LDA given by $[w_{face_1}, w_{face_2}, \dots, w_{face_n}]$ and Y_{finger} be the feature vector of fingerprint extracted using HOG given by $[w_{finger_1}, w_{finger_2}, \dots, w_{finger_n}]$ where n is the number of training samples or test samples. A new feature vector is generated by serially concatenating face feature, Y_{face} and its corresponding fingerprint feature, Y_{finger} . The combination of both feature vectors becomes $[w_{face_1}, w_{face_2}, \dots, w_{face_n}, w_{finger_1}, w_{finger_2}, \dots, w_{finger_n}]$. These combined features are given for SVM for classification.

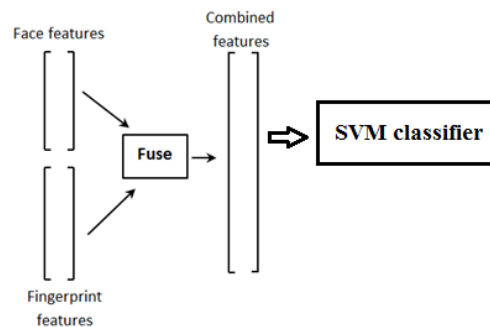


Figure 6. Feature Fusion Using Concatenation Method

V. PROPOSED STRUCTURE FOR COMBINING MATCHING SCORE LEVEL AND FEATURE LEVEL

A multimodal biometric system has been developed using face and fingerprint with the information fusion at matching score level and feature level. Matching score level fusion has been used for verification purpose and feature level fusion is used for recognition purpose. Whenever the query face and fingerprint comes for authentication, they are checked for their existence in the database, if they exist then the system proceeds for identification stage. The data flow in our proposed multimodal biometric system is shown in Fig. 7.

In order to authenticate a user, the scores of the query face and fingerprint images are computed. Fingerprint results in similarity scores and face results in distance scores. Hence the scores are transformed into common domain using min-max normalization technique which transforms the scores between $\{0,1\}$. Now the normalized face and fingerprint scores are fused using the combination approach where the weighted sum rule has been used for fusion. After calculating the final scores of face and fingerprint for both genuine and imposter, the threshold has been set which clearly discriminates the scores of the imposter and scores of genuine. If the query face and fingerprint are found to be genuine (i.e., found in the database) then the features extracted from the query face and fingerprint are subjected for fusion at feature level, if not, modalities are rejected by labeling

them as unauthorized user. The multi-class support vector machine (SVM) has been used for classification, it takes the input data and labels each one of samples as either belonging to a given class or not.

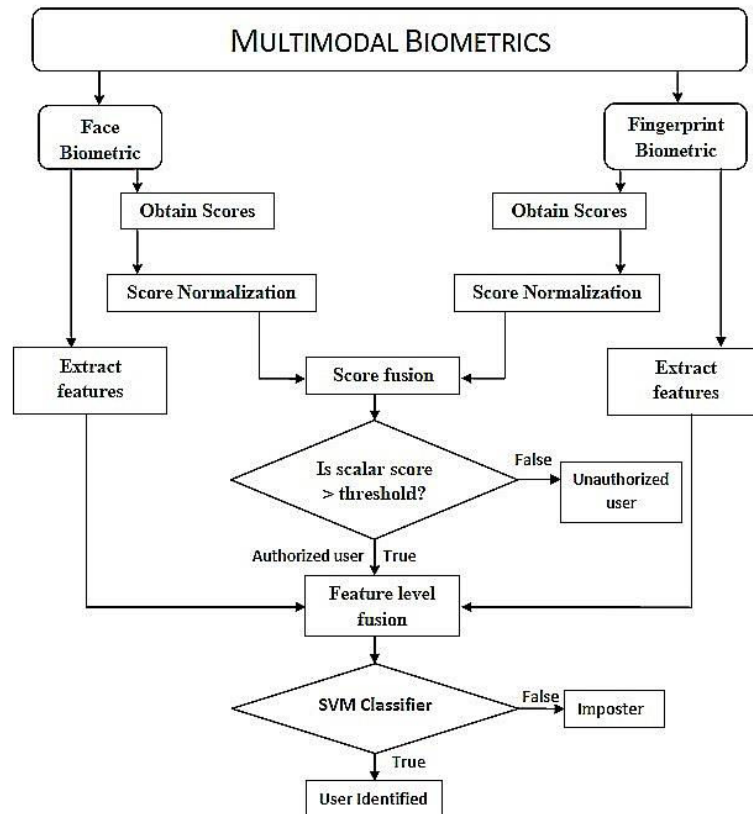


Figure 7. Data flow of the Proposed Multimodal Biometric System

IV. EXPERIMENTAL RESULTS

In this section, we have presented the experimental results of the proposed methodology. The algorithm is implemented using Matlab 2013. The proposed work has been carried out using PC Intel core i3 2nd generation CPU @ 2.2GHz processor and 4GB RAM. The database used for fingerprint consists of 10 images / subject for training and 5 images / subject for testing of 20 subjects. The database used for face consists of 15 images / subject for training with illumination and pose variation and 5 images / subject for testing of the same 20 subjects. The accuracy of individual biometric modality is low but the combination of modalities results in superior accuracy.

Table 1. Comparison of Accuracy of Different Modalities Using Score Level Fusion

Biometric Modalities	FRR	FAR	Accuracy
Face	23%	16%	80.5%
Fingerprint	8%	25%	83.5%
Face + Fingerprint using weighted sum rule	9%	19%	86%

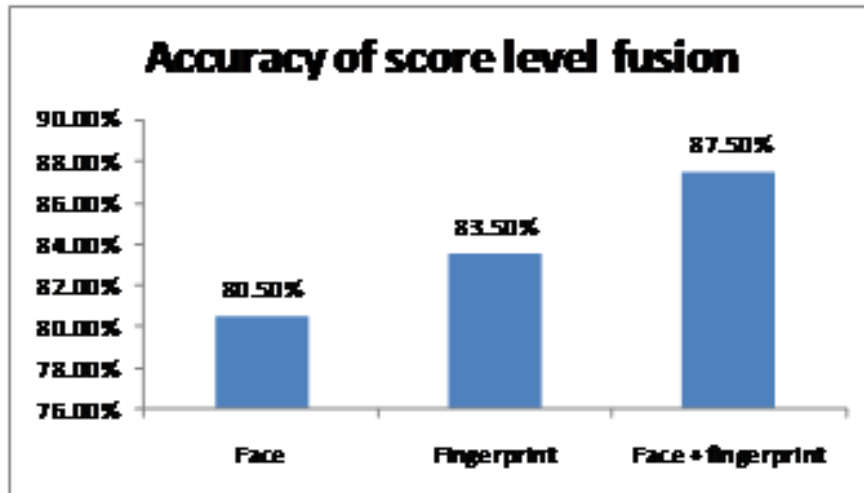


Figure 8. Comparison of Accuracy of Different Modalities Using Score Level Fusion

The individual accuracy of face with Euclidean distance classifier is 84.6% and accuracy of fingerprint with SVM classifier is 85%. The accuracy of fusion at feature level is 93.6%.

Table 2. Comparison of Accuracy of Different Modalities Using Feature Level Fusion

Biometric Modalities	Accuracy
Face	84.6%
Fingerprint	85%
Face + Fingerprint using concatenation method	93.6%

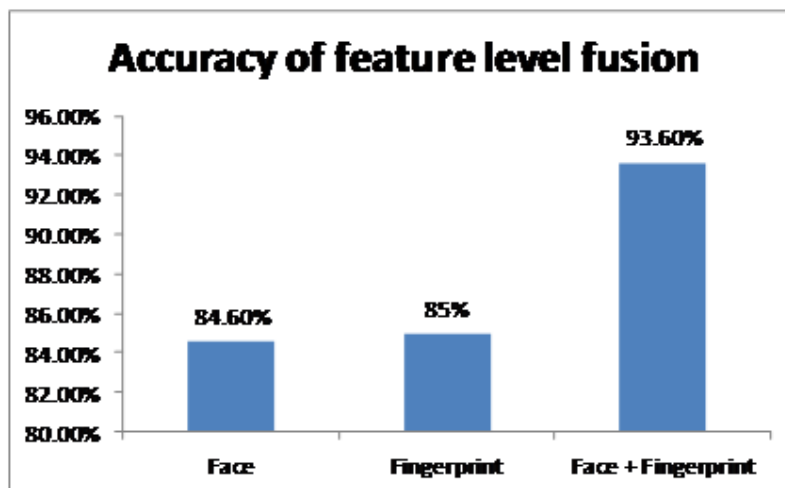


Figure 9. Comparison of Accuracy of Different Modalities Using Feature Level Fusion

VII. CONCLUSION

In this paper we have proposed a multimodal biometric system with fusion at score level and feature level for face and fingerprint. It is evident from the experimental results that multimodal biometric systems outperform unimodal biometric systems and also the recognition performance has improved when compared to individual biometric system. The main contribution of this paper is to develop a multimodal biometric system which

reduces the FRR and FAR. This authentication system is robust to variations in illumination and posture. Also it can deal with noisy sensor data, non-universality and spoofing problems efficiently and effectively.

Further work of authentication can be improved significantly by integrating other biometrics into the system.

REFERENCES

- [1] P. S. Sanjekar and J. B. Patil, "An Overview of Multimodal biometrics", Signal & Image Processing: An International Journal (SIPIJ), Vol.4, No.1, February 2013.
- [2] L. Hong, A. K. Jain, and S. Pankanti, "Can Multibiometrics Improve Performance?" , In Proceedings of IEEE Workshop on Automatic Identification Advanced Technologies, pp: 59-64, New Jersey, U.S.A., October 1999.
- [3] Arun Ross and Anil K. Jain, "Multimodal Biometrics: An Overview", Proc. Of 12th European Signal Processing Conference (EUSIPCO), (Vienna, Austria), pp. 1221-1224, September 2004.
- [4] A. K. Jain and A. Ross, "Multibiometric Systems", Communications of the ACM, Special Issue on Multimodal Interfaces, 47(1), pp:34-40, January 2004.
- [5] Arun Ross, Anil. K. Jain, "Information fusion in biometrics", Elsevier, Pattern Recognition Letters 24, pp: 2115-2125, March 2003.
- [6] Hassan Soliman, "Feature level fusion of Palm veins and Signature Biometrics", International Journal of video & Image Processing and Network Security, IJVIPNS-IJENS, vol:12, no.01,2006
- [7] Rattani.A, Kisku.D.R, Bicego.M, and Tistarelli.M, "Feature level fusion of face and fingerprint biometrics", In proc. Of 1st IEEE international conference on biometrics: Theory, applications and systems, pp. 1-6, Washington DC, USA.
- [8] Sumeet Kaur, Priyanka Sharma, "Analysis of Multimodal Biometrics at Feature Level using face and palmprint", International Journal of Advanced Research in Computer Science and Software Engineering, Volume 3, Issue 7, July 2013.
- [9] Maya V. Karki, Dr. S. Sethu Selvi, "Multimodal Biometrics at Feature Level Fusion using Texture Features", International Journal of Biometrics and Bio-informatics (IJBB), Volume (7) : Issue (1), 2013.
- [10] Feifei Cui, Gongping Yang, "Score Level Fusion of Fingerprint and Finger Vein Recognition", Journal of Computational Information Systems 7: 16, pp: 5723-5731, 2011.
- [11] Priyanka S. Patil, A. S. Abhyankar, "Multimodal Biometric Identification System Based On Iris & Fingerprint", IOSR Journal of VLSI and Signal Processing (IOSR-JVSP), Volume 1, Issue 6, PP 76-83, April 2013.
- [12] Youssef Elmir, Zakaria Elberrichi, Reda Adjoudj, "Score level fusion based multimodal biometric system", Science of Electronics technologies of Information and Telecommunications (SETIT), March 2014, Tunisia.
- [13] Paul Viola, Michael J. Jones, "Robust Real-Time Face detection" International Journal of Computer Vision 57(2), 137–154, 2004.